The Plant Cell, Vol. 32: 374–391, February 2020, www.plantcell.org © 2020 ASPB.

Nup96 and HOS1 Are Mutually Stabilized and Gate CONSTANS Protein Level, Conferring Long-Day Photoperiodic Flowering Regulation in Arabidopsis[CC-BY]

Zhiyuan Cheng,[a,1] Xiaomei Zhang,[a,1] Penghui Huang,[a,1] Guowen Huang,[a,b,1] Jinglong Zhu,[a] Fulu Chen,[a] Yuchen Miao,[c] Liangyu Liu,[d,2] Yong-Fu Fu,[a,2] and Xu Wang[a,2]

[a] Ministry of Agriculture Key Laboratory of Soybean Biology (Beijing), National Key Facility of Crop Gene Resource and Genetic Improvement, Institute of Crop Sciences, Chinese Academy of Agricultural Sciences, Beijing 100081, China
[b] Department of Chemical Sciences and Biological Engineering, Hunan University of Science and Technology, Yongzhou 425100, Hunan, China
[c] Key Laboratory of Plant Stress Biology, State Key Laboratory of Cotton Biology, School of Life Sciences, Henan University, Kaifeng 475004, China
[d] College of Life Sciences, Capital Normal University, Beijing 100048, China

ORCID IDs: 0000-0002-1326-2179 (Z.C.); 0000-0002-5816-3895 (X.Z.); 0000-0003-0197-4846 (P.H.); 0000-0003-4314-0890 (G.H.); 0000-0002-3130-6702 (J.Z.); 0000-0002-9856-0027 (F.Z.); 0000-0002-4339-1238 (Y.M.); 0000-0002-8250-934X (L.L.); 0000-0001-7339-263X (Y.F.); 0000-0003-2210-6204 (X.W.).

The nuclear pore complex profoundly affects the timing of flowering; however, the underlying mechanisms are poorly understood. Here, we report that *Nucleoporin96* (*Nup96*) acts as a negative regulator of long-day photoperiodic flowering in Arabidopsis (*Arabidopsis thaliana*). Through multiple approaches, we identified the E3 ubiquitin ligase HIGH EXPRESSION OF OSMOTICALLY RESPONSIVE GENE1 (HOS1) and demonstrated its interaction in vivo with Nup96. Nup96 and HOS1 mainly localize and interact on the nuclear membrane. Loss of function of *Nup96* leads to destruction of HOS1 proteins without a change in their mRNA abundance, which results in overaccumulation of the key activator of long-day photoperiodic flowering, CONSTANS (CO) proteins, as previously reported in *hos1* mutants. Unexpectedly, mutation of *HOS1* strikingly diminishes Nup96 protein level, suggesting that Nup96 and HOS1 are mutually stabilized and thus form a novel repressive module that regulates CO protein turnover. Therefore, the *nup96* and *hos1* single and *nup96 hos1* double mutants have highly similar early-flowering phenotypes and overlapping transcriptome changes. Together, this study reveals a repression mechanism in which the Nup96-HOS1 repressive module gates the level of CO proteins and thereby prevents precocious flowering in long-day conditions.

INTRODUCTION

Plants have evolved the ability to sense various environmental signals, such as seasonal daylength and temperature changes, that determine the optimal timing of flowering for successful reproduction (Michaels, 2009; de Montaigu et al., 2010; Jarillo and Piñeiro, 2011). In Arabidopsis (*Arabidopsis thaliana*), the prevailing molecular mechanism of daylength perception includes circadian clock-controlled transcription and proteasome-dependent protein degradation of the transcription factor CONSTANS (CO). Through these mechanisms, CO proteins are confined to accumulate at dusk in long days (Samach et al., 2000; Valverde et al., 2004; Shim et al., 2017). The accumulated CO proteins directly activate the transcription of the "florigen" gene *FLOWERING LOCUS T* (*FT*) in leaves, whose coding protein is transported to the apex and in turn induces the expression of floral meristem identity genes, such as *APETALA1* and *LEAFY*, to initiate the formation of floral primordia (Weigel et al., 1992; Abe et al., 2005; Wigge et al., 2005). *CO* transcription is tightly controlled by manifold positive and negative regulators. Two different groups of transcription factors, *FLOWERING BHLH* (*FBH*) and *TEOSINTE BRANCHED1/CYCLOIDEA/PROLIFERATING CELL NUCLEAR ANTIGEN FACTOR* (*TCP*), are activators of *CO*, through directly binding to the *CO* promoter (Ito et al., 2012; Kubota et al., 2017). Both FBH1 and TCP4 physically interact with another *CO* gene activator, GIGANTEA (GI; Koornneef et al., 1998; Suárez-López et al., 2001; Kubota et al., 2017), but the functional dependency of FBH1 and TCP4 on GI is different. TCP4 activates *CO* in a GI-dependent manner, whereas FBH1 is partially independent of GI to activate *CO* (Kubota et al., 2017). *CO* expression can also be repressed by CYCLING DOF FACTOR proteins, which are able to bind DOF binding sites in the *CO* promoter (Imaizumi et al., 2005; Fornara et al., 2009). In addition to transcriptional regulation, posttranslational regulation of CO is also essential for measuring daylength. The best characterized posttranslational regulation of CO proteins is proteasome-dependent degradation, which utilizes different E3 ubiquitin ligases. The E3 ligase CONSTITUTIVE

[1] These authors contributed equally to this work.
[2] Address correspondence to liangyu.liu@cnu.edu.cn, fuyongfu@caas.cn, and wangxuen@gmail.com.
The author responsible for distribution of materials integral to the findings presented in this article in accordance with the policy described in the Instructions for Authors (www.plantcell.org) is: Yong-Fu Fu (fuyongfu@caas.cn).

www.plantcell.org/cgi/doi/10.1105/tpc.19.00661

PHOTOMORPHOGENIC1 (COP1) associates with *SUPPRESSOR of phyA-105* to specifically degrade CO proteins in the dark (Jang et al., 2008), while another E3 ligase, HIGH EXPRESSION OF OSMOTICALLY RESPONSIVE GENE1 (HOS1), mediates the degradation of CO in the morning in long days (Jung et al., 2012; Lazaro et al., 2012). Other mechanisms have also been implicated in the direct stabilization of CO proteins (Song et al., 2012, 2014).

Although numerous genes have been identified so far in flowering time regulation, the underlying molecular mechanisms for many of them are poorly understood. One example is a group of nuclear pore-associated proteins. The nuclear pore complex is embedded in the nuclear envelope, the physical barrier separating the nucleus from the cytosol, and serves as the sole channel for nucleocytoplasmic transportation of macromolecules (i.e., proteins and RNAs; Meier and Brkljacic, 2009; Wälde and Kehlenbach, 2010). The nuclear pore complex is composed of multiple copies of ~30 different nucleoporins (Nups), which form several subcomplexes (Tran and Wente, 2006; Strambio-De-Castillia et al., 2010). In Arabidopsis, most Nups have been identified so far by genetic and biochemical approaches (Tamura et al., 2010), and some of them are reported to participate in various important developmental and resistant processes. Mutations of *Nup136* (also known as *Nup1*), *Nup160* (also known as *SUPPRESSOR OF AUXIN RESISTANCE1* [*SAR1*]), *Nup96* (*SAR3* or *MODIFIER OF SNC1,3* [*MOS3*]), and *AtTPR* (*Arabidopsis thaliana TRANSLOCATED PROMOTER REGION*, also known as *NUCLEAR PORE ANCHOR*) significantly promote flowering of plants (Zhang and Li, 2005; Parry et al., 2006; Jacob et al., 2007; Xu et al., 2007; Tamura et al., 2010; Parry, 2014), while plants deficient in *Nup62*, *Nup58*, and *Nup54* gene functions manifest moderately early-flowering phenotypes (Zhao and Meier, 2011; Parry, 2014; Boeglin et al., 2016). Moreover, loss of function of some proteins partially distributed on the nuclear envelope also leads to an altered flowering time of plants. For example, the *low expression of osmotically responsive genes4* (Gong et al., 2005), *early in short days4* (Murtas et al., 2003), and *hos1* (Jung et al., 2012, 2013; Lazaro et al., 2012) mutants display early-flowering phenotypes. This evidence strongly suggests that nuclear pore-associated proteins play fundamental roles in regulating flowering time in Arabidopsis. However, until now, there was no detailed evidence about the underlying molecular mechanism confirming that Nups regulate flowering.

In this study, we show that one component of the nuclear pore complex, *Nup96*, negatively regulates the transition to flowering in Arabidopsis. By combining a proteomic approach with a protein-protein interaction analysis, we demonstrate that flowering repressor HOS1 E3 ligase associates with Nup96 in vivo at the nuclear envelope. Loss of function of *Nup96* leads to the destruction of HOS1 proteins, which results in invariable phenotypes of the *nup96* and *hos1* single and the *nup96 hos1* double mutants in flowering time. As previously reported in *hos1* mutants (Lazaro et al., 2012), the early flowering of *nup96* mutants could be largely explained by an overaccumulation of CO proteins. Moreover, an unexpected reduction of the Nup96 protein level in *hos1* mutants has been observed in this study. Together, these results uncover a mechanism through which the mutually stabilized Nup96-HOS1 repressor complex negatively regulates CO abundance and prevents precocious flowering of Arabidopsis in long-day conditions.

RESULTS

Nup96 Acts as a Negative Regulator of Flowering in Arabidopsis

In human cells, Nup96 and Nup98 are encoded as one fusion gene and synthesized as a 186-kD precursor protein. Autoproteolytic cleavage of this precursor releases two mature nucleoporins, Nup96 and Nup98 (Fontoura et al., 1999). By contrast, Arabidopsis *Nup96* (*SAR3/MOS3*, At1g80680) and *Nup98* (*Nup98a*, At1g10390; *Nup98b*, At1g59660) genes reside in separate loci in the genome and are synthesized into proteins individually (Zhang and Li, 2005; Parry et al., 2006; Tamura et al., 2010). Noticeably, the well-conserved Autoproteolytic Processing Domain (APD) is retained in both Nup96 and Nup98 proteins in Arabidopsis (Figure 1A). Nup96 proteins from most plant species investigated present structures similar to Arabidopsis Nup96 with the conserved APD (Supplemental Figure 1; Supplemental Data Set 1), suggesting that *Nup96* genes diversified independently in plant and animal lineages. Previous characterization of *Nup96* in Arabidopsis has shown its crucial roles in auxin signaling and the immune response (Zhang and Li, 2005; Parry et al., 2006); although observations suggested that the *nup96* mutation caused early flowering of plants (Parry et al., 2006), the underlying molecular mechanisms remained unknown.

To address this question, we first recharacterized the flowering phenotypes of two mutant alleles, *nup96-1* (SALK_109959, also known as *sar3-3* or *mos3-2*; Zhang and Li, 2005; Parry et al., 2006) and *nup96-2* (SALK_117966, also known as *mos3-3*; Zhang and Li, 2005; Figure 1B) under various experimental conditions. Using RT-PCR and immunoprecipitation (IP) assays, we verified that both alleles were null, as no full-length *Nup96* transcripts and proteins could be detected (Figures 1C and 1D). When grown under long-day or short-day conditions, both *nup96-1* and *nup96-2* mutants flowered much earlier than wild-type plants (Figures 1B and 1E), suggesting that *Nup96* negatively regulates the transition to flowering in Arabidopsis. We also noticed that *nup96* mutants flowered much earlier in long days than in short days, indicating a limited effect of *Nup96* mutation on the plant's sensitivity to daylength change. Next, we observed complementation of the early-flowering phenotype (Figures 1F and 1G) when *nup96-1* plants were transformed with either *Nup96* cDNA driven by a cauliflower mosaic virus 35S promoter or a *Nup96-GFP* fusion gene driven by a 2.5-kb promoter upstream of the *Nup96* coding sequence, which produced normal Nup96 proteins (Figure 1H). This observation corroborated the notion that early flowering of *nup96* mutants was indeed due to the loss of *Nup96* function.

Evolutionarily Conserved Autoproteolytic Processing Is Not Required for the Flowering Activities of Nup96

Considering that a conserved proteolytic cleavage site is located at the N terminus of Nup96 (Fontoura et al., 1999; Iwamoto et al., 2010), we wondered whether this site was active and necessary for the flowering functions of Nup96. To this end, we created mutated Nup96 proteins in which either the Phe (F187) and Ser (S188) residues in the cleavage domain (HFS, the nucleoporin2 domain in animals and yeast with pfam accession number PF04096 [Fontoura et al., 1999; Iwamoto et al., 2010]) were mutated to Gln (F187Q) and

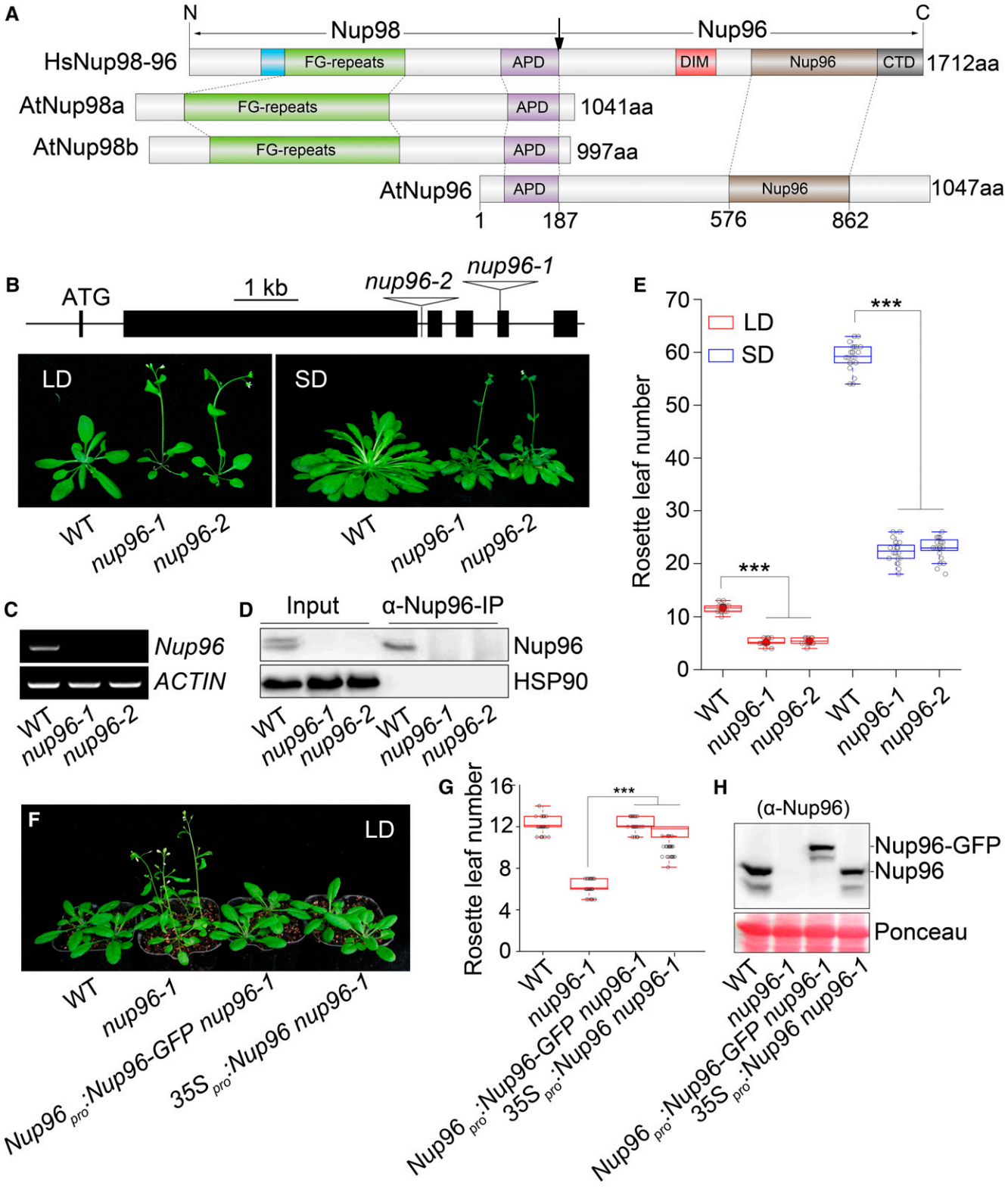

Figure 1. *Nup96* Acts as a Negative Regulator of Flowering in Arabidopsis.

(A) Domain structures of human Nup98-96 (HsNup98-96), Arabidopsis Nup98a and Npu98b (AtNup98a and AtNup98b), and Arabidopsis Nup96 (AtNup96). Domains are indicated as follows: the GLEBS motif (blue), the Phe-Gly repeat region (FG-repeats; green), the APD (purple), the domain invasion motif (DIM;

Ala (S188A), respectively, or APD (the first 187 residues) in the N terminus was deleted (*Nup96*$^{\Delta 187}$; Figure 2A). Then, the wild-type *Nup96*, *Nup96*$^{F187Q,\ S188A}$ (*Nup96m*), and *Nup96*$^{\Delta 187}$ (*Nup96ΔN*) genes were fused with the *GFP* coding sequence and expressed under the control of the 2.5-kb *Nup96* promoter region (*Nup96*$_{pro}$) in the *nup96-1* background. These plants are hereafter referred to as *Nup96-GFP*, *Nup96m-GFP*, and *Nup96ΔN-GFP*, respectively (Figure 2A). We reasoned that if the cleavage site was active in plants, the first 187 residues from the N-terminal end of Nup96 proteins would be removed. Therefore, the *Nup96-GFP* and *Nup96ΔN-GFP* transgenes should be able to produce identical proteins that are ~20 kD smaller (~125 kD) than the predicted size of Nup96-GFP (~145 kD). Indeed, using an immunoblot assay, we detected recombinant proteins that were slightly smaller than 130 kD in both *Nup96-GFP* and *Nup96ΔN-GFP* plants. By contrast, a protein product larger than 130 kD was detected in *Nup96m-GFP* plants (Figure 2B). A similar observation was made in wild-type plants. Using an anti-Nup96-specific antibody raised in this study, which recognizes the C terminus of Nup96 (amino acids 550–900), we found that in wild-type plants, Nup96 proteins existed as an ~100-kD form rather than the predicted 119-kD proteins (Figure 2B). These results suggested that Nup96 proteins undergo proteolytic processing in plants by removing a short fragment from its N-terminal end.

We next investigated whether the proteolytic processing was necessary for the flowering-repression activity of Nup96 using flowering time as the readout. We observed that the early-flowering phenotype of *nup96-1* mutants could be fully rescued by expressing *Nup96-GFP*, *Nup96m-GFP*, and *Nup96ΔN-GFP* transgenes (Figures 2C and 2D), and limited phenotypic variability was found among those plants. Furthermore, we examined the subcellular distributions of Nup96-GFP, Nup96m-GFP, and Nup96ΔN-GFP proteins in plant roots. All three versions of the proteins concentrated on the nuclear envelope, and no distinguishable patterns were observed (Figure 2E). Taken together, these data suggested that the proteolytic removal of the N-terminal residues was not required for the nuclear envelope-targeting and floral regulatory activities of Nup96 proteins in Arabidopsis.

Nup96 Regulates Flowering through Modulating the Expression of Floral Integrator Genes

To dissect the molecular basis contributing to the early flowering of *nup96-1* mutants, we first profiled the expression patterns of floral integrator genes *FT* and *SUPPRESSOR OF OVEREXPRESSION OF CONSTANS1* (*SOC1*) in both the wild type and *nup96-1* mutants by qPCR. *FT* and *SOC1* expression increased during the development of wild-type and *nup96-1* seedlings grown in long days; however, both genes showed higher levels in *nup96-1* on day 11 after germination (Figure 3A) when floral transition occurred (Shen et al., 2011). Then, we compared the daily expression patterns of *FT* and *SOC1* in the wild type and *nup96-1* mutants under different daylengths. The overall levels of transcripts for both genes were higher in *nup96-1* than in wild-type plants, but the degrees varied among time points (Figure 3B). For example, in long days, *FT* appeared more abundant in the morning (Zeitgeber time 4 [ZT4]) in *nup96-1* than in wild-type plants, while the level of *SOC1* transcript remained higher in *nup96-1* than in the wild type from noon until the end of the day (Figure 3B). These observations suggested that the early flowering of *nup96* mutants was quite likely due to the upregulation of floral integrator genes. This notion was further supported by the observation that both *nup96-1 ft-1* and *nup96-1 soc1-2* double mutants flowered much later than *nup96-1* single mutants (Figures 3C and 3D). However, it is worth noting that the *ft* mutation was much more effective than *soc1* in terms of delaying the flowering of *nup96* mutants in long days, suggesting that the elevated *FT* expression might be the major cause leading to the accelerated flowering of *nup96* mutants in long days.

It has been reported that the activation of *FT* mRNA expression mostly occurs in the leaf phloem companion cells (An et al., 2004). Given that Nup96 adversely regulated *FT* expression (shown above), it was likely to share a similar spatial expression pattern to *FT*. Therefore, we examined the spatial expression of *Nup96* in transgenic plants expressing the GUS reporter driven by the *Nup96* native promoter (*Nup96*$_{pro}$). *Nup96* was ubiquitously expressed throughout the plant, including the leaf vasculature, shoot apical meristem, roots, reproductive organs, and other tissues (Supplemental Figure 2A). This broad expression of *Nup96* was consistent with the published transcriptomic data (Supplemental Figure 2B) and the diverse developmental abnormalities of *nup96* mutants (Supplemental Figures 2C–2L).

Nup96 Interacts with HOS1 in Plants

To investigate the molecular mechanisms by which *Nup96* prevents plants from precocious flowering, we purified Nup96 protein

Figure 1. (continued).

red), the Nup96 domain (Nup96; brown), and the C-terminal domain (CTD; gray). The vertical arrow indicates the sites of autoproteolytic cleavage. aa, Amino acids.

(B) Scheme of *Nup96* gene structure showing the positions of two T-DNA insertions (*nup96-1* and *nup96-2*) and flowering phenotypes of the wild type (WT) and *nup96-1* and *nup96-2* mutants under long-day (LD) and short-day (SD) conditions. Black lines indicate introns. Black bars represent exons. Star codon ATG is indicated. Triangles refer to T-DNAs.

(C) RT-PCR analysis of *Nup96* full-length transcripts in different genotypes. *ACTIN* was used as the control. WT, wild type.

(D) IP assay of Nup96 proteins in different genotypes. WT, wild type.

(E) Measurement of rosette leaf numbers of different genotypes ($n > 20$). Asterisks indicate significant differences according to Student's *t* test (***, $P < 0.001$). WT, wild type.

(F) Flowering phenotypes of the wild type, *nup96-1*, and two complementation lines. WT, wild type.

(G) Measurement of rosette leaf numbers of genotypes shown in **(F)**; $n > 20$. Asterisks indicate a significant difference according to Student's *t* test (***, $P < 0.001$). WT, wild type.

(H) Immunoblot showing protein levels of endogenous Nup96 and Nup96-GFP in genotypes shown in **(F)** using anti-Nup96 antibodies. WT, wild type.

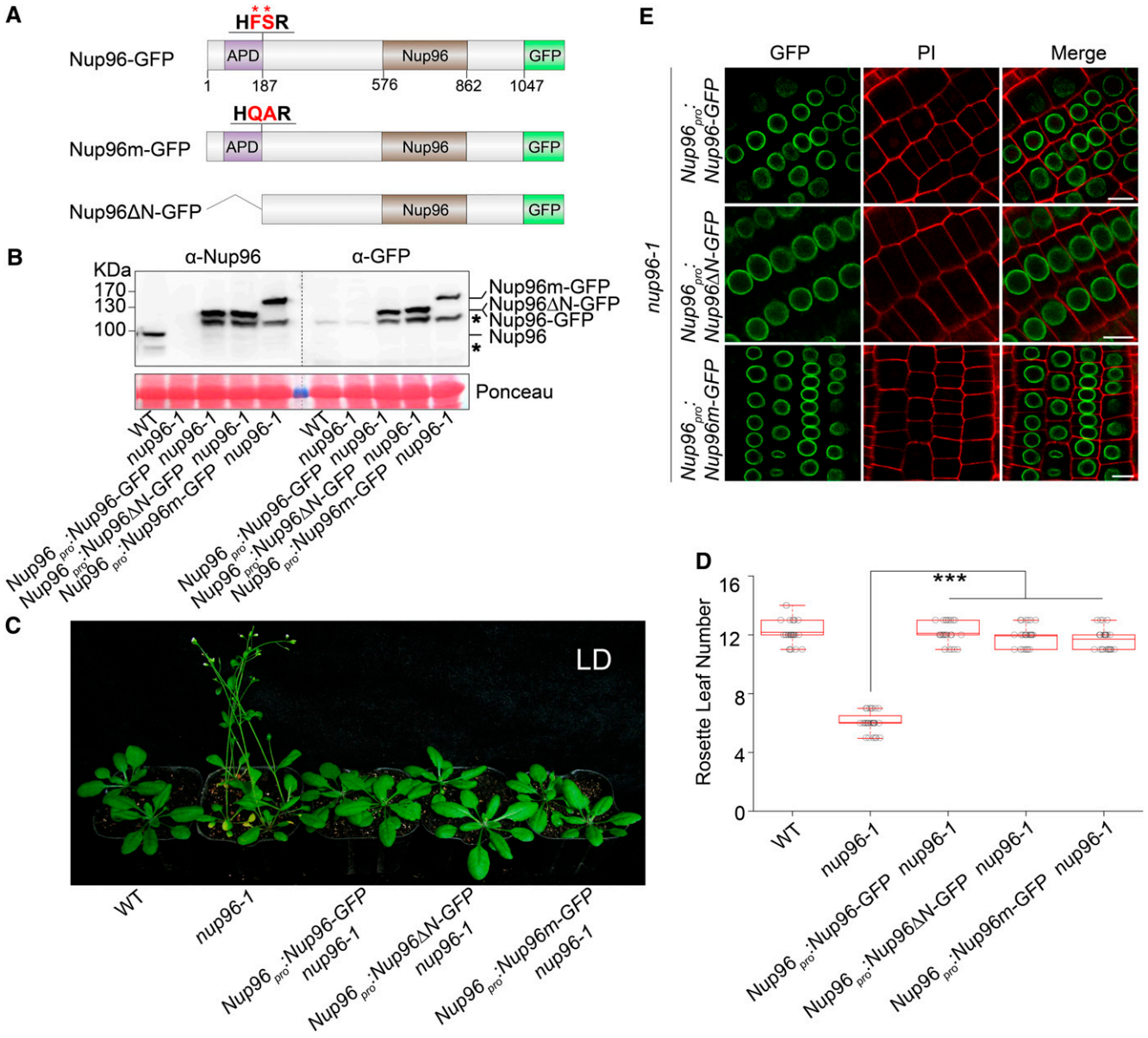

Figure 2. Autoproteolytic Processing Is Not Required for the Physiological Activities of Nup96.

(A) Domain structures of Nup96-GFP, Nup96m-GFP, and Nup96ΔN-GFP fusion proteins. Domains of Nup96 are indicated as follows: the APD (purple box), the Nup96 domain (Nup96; brown box), and the rest of the regions (white box). The GFP fused to different versions of Nup96 are shown as a green box. The autoproteolytic cleavage site is shown as "HFSR," and the key residues (F and S) used for mutations are labeled by asterisks and highlighted as red color. The numbers below the Nup96-GFP structure denote the positions in the amino acid sequence.

(B) Immunoblots showing the levels of endogenous Nup96, Nup96-GFP, Nup96m-GFP, and Nup96ΔN-GFP proteins in plants shown in **(C)** detected by anti-Nup96 and anti-GFP antibodies. Asterisks denote unknown bands. WT, wild type.

(C) Flowering phenotypes of the wild type, *nup96-1*, and transgenic lines expressing the proteins indicated in **(A)**. WT, wild type.

(D) Rosette leaf numbers of genotypes shown in **(C)** at the time of flowering ($n > 20$). Box plots are used to display the distributions of data points (presented as circles). The lines in the box (from top to bottom) indicate the maximum, third quartile, mean, first quartile, and minimum. Asterisks indicate a significant difference according to Student's *t* test (***, $P < 0.001$). WT, wild type.

(E) Subcellular distributions of Nup96-GFP, Nup96m-GFP, and Nup96ΔN-GFP fusion proteins indicated in **(A)** in plant root cells. Bars = 10 μm.

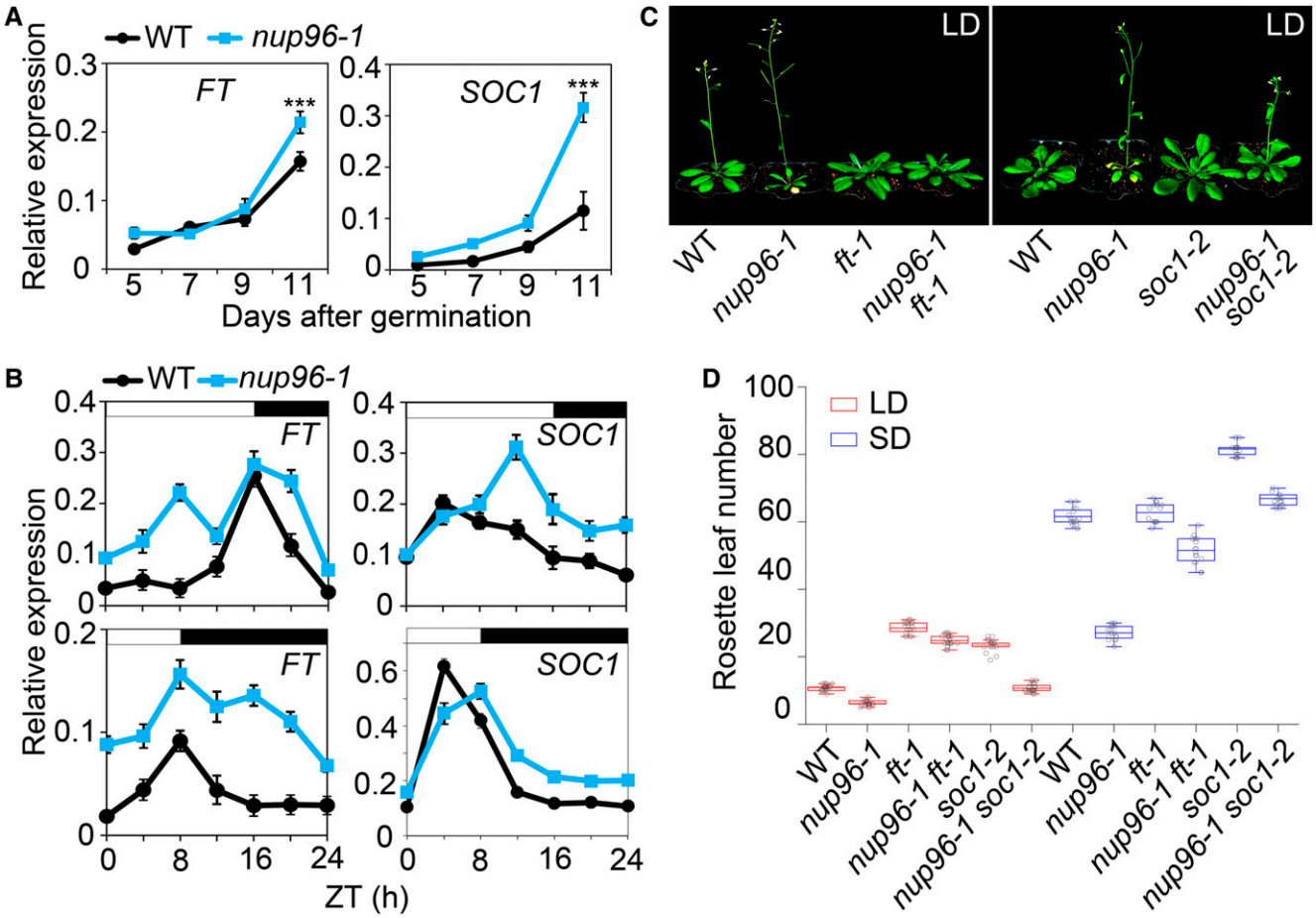

Figure 3. *Nup96* Regulates Flowering through Modulating the Expression of Floral Integrator Genes.

(A) qPCR analysis of *FT* and *SOC1* expression in the wild type (WT) and *nup96-1* mutants grown in long days for the indicated periods after germination. Values are means ± SD ($n = 3$ biological repeats). ***, $P < 0.001$.

(B) Diurnal expression of *FT* and *SOC1* in wild-type and *nup96-1* seedlings grown in long-day and short-day conditions for 9 d. Values are means ± SD ($n = 3$ biological repeats). White bars indicate day, and black bars represent night. WT, wild type.

(C) Flowering phenotypes of the indicated genotypes in long days. WT, wild type.

(D) Rosette leaf numbers at the time of flowering for the genotypes shown in **(C)**; $n > 20$. Box plots are used to display the distributions of data points (presented as circles). The lines in the box (from top to bottom) indicate the maximum, third quartile, mean, first quartile, and minimum. WT, wild type.

complexes from *Nup96-GFP/nup96-1* plants by IP using GFP affinity chromatography (Rothbauer et al., 2008), and the protein complexes were then analyzed by mass spectrometry (MS). The Nup96-GFP fusion proteins in the transgenic line we used showed comparable levels to endogenous Nup96 proteins in wild-type plants (Figures 1H and 2B). GFP-only overexpression plants were analyzed in parallel in IP-MS experiments as the negative control (Figure 4A). After excluding those identified by MS in GFP-only samples, we found that different groups of nucleoporins were specifically coprecipitated with Nup96-GFP from plant protein extracts (Figure 4B), indicating a strong association of Nup96 with other components of the nuclear pore complex. An important flowering repressor, HOS1 (Figure 4B; Jung et al., 2012; Lazaro et al., 2012), which is a RING-type E3 ubiquitin ligase and shares homology with yeast and human nucleoporin EMBRYONIC LARGE MOLECULE DERIVED FROM YOLK SAC protein (Tamura et al., 2010; Bilokapic and Schwartz, 2013), was among these proteins (Figure 4B).

To verify the in vivo association of HOS1 and Nup96, we first examined if the two proteins had overlapping distributions in plant cells. Transgenic plants were prepared to independently express the genomic sequence of *HOS1* including a 2-kb promoter region, the coding region fused with the *mCherry* open reading frame (*gHOS1-mCh*), and the entire *Nup96* genomic DNA (a 2.2-kb promoter region was included) fused with the coding sequence of *GFP* (*gNup96-GFP*). Then, the dual expression lines were obtained by crossing *gHOS1-mCh* with *gNup96-GFP* plants. In agreement with the previous studies (Parry et al., 2006; Lazaro et al., 2012), we observed that both HOS1-mCherry and Nup96-GFP proteins dominantly located at the nuclear envelope either in single or dual transgenic plants (Figure 4C).

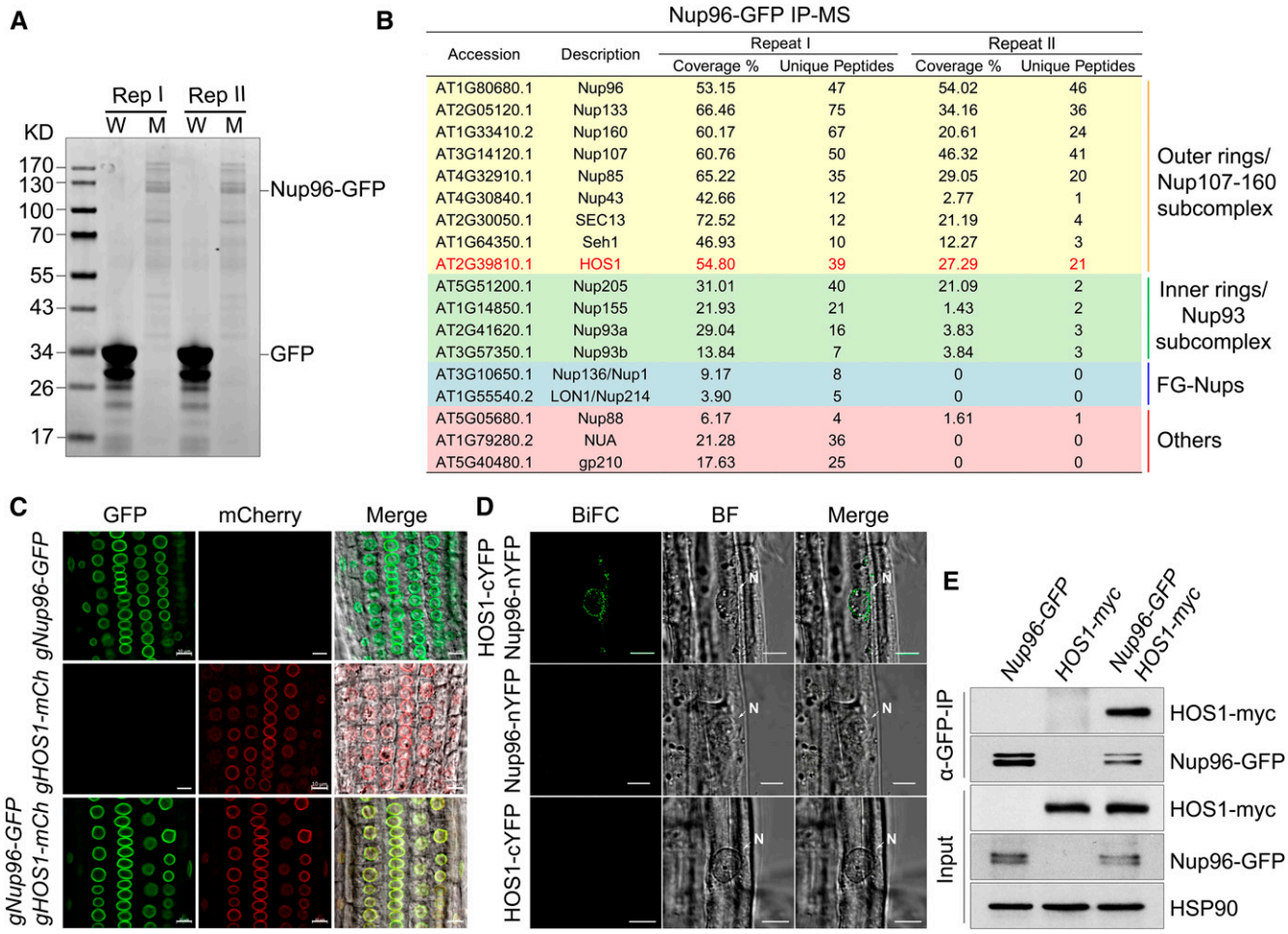

Figure 4. Nup96 Interacts with HOS1 in Plants.

(A) Coomassie Brilliant Blue staining of proteins immunoprecipitated by GFP-trap from the lysates of *35S:GFP* wild-type (W) and *Nup96-GFP nup96-1* (M) plants grown in long-day conditions for 9 d. Two replicates (Rep I and Rep II) were performed.
(B) Identification of the Nup96 complex by MS. HOS1 is highlighted by red color.
(C) Colocalization of Nup96-GFP and HOS1-mCherry in transgenic plant roots. Bars = 10 μm.
(D) BiFC assay showing the interaction of Nup96 and HOS1 in transgenic plants. BF, bright field. Bars = 20 μm.
(E) Co-IP assay showing the in vivo interaction of Nup96 and HOS1 in transgenic plants. GFP-trap was used to isolate Nup96-GFP from plant protein extracts, and HOS1-myc was then detected in the immunoprecipitates by anti-myc antibodies. HSP90 was used as the loading control for the input samples.

Next, we examined whether the two proteins interact with each other at the nuclear envelope using a bimolecular fluorescence complementation (BiFC) assay. We separately transformed wild-type plants with *35S:Nup96-nYFP* (*nYFP*, N-terminal end of YFP) and *35S:HOS1-cYFP* (*cYFP*, C-terminal end of YFP), then the two transgenes were brought together by genetic cross. We found that the BiFC signal was strongly enriched at the nuclear envelope in the double transgenic line (Figure 4D), suggesting that Nup96 and HOS1 indeed interact at the nuclear envelope. Finally, we performed a coimmunoprecipitation (co-IP) assay to detect the interaction of Nup96 and HOS1 in plants. We expressed two transgenes of *HOS1-myc* and *Nup96-GFP* simultaneously in plants resulting from the genetic cross of the transgenic line expressing *35S:HOS1-myc* and the *Nup96-GFP nup96-1* complementation line. Using anti-GFP antibodies, HOS1-myc proteins were successfully copurified with Nup96-GFP from the lysate of dual transgenic plants (Figure 4E), reflecting the coexistence of Nup96 and HOS1 in common protein complexes. In summary, our results demonstrate that the floral repressor Nup96 associates with HOS1 at the nuclear envelope in Arabidopsis.

Nup96 and HOS1 Are Mutually Stabilized in Plants

To evaluate how loss of function of *Nup96* influences the activities of *HOS1*, we first investigated if the transcription of *HOS1* was altered in *nup96* mutants. qPCR results revealed that *HOS1* expression was slightly elevated in *nup96-1* mutants compared with that in wild-type plants (Figure 5A), suggesting that *Nup96* mutation has limited effects on *HOS1* expression. Next, we examined HOS1 protein levels in different genotypes using anti-HOS1 antibodies,

which clearly detected endogenous HOS1 proteins in wild-type plants. However, we surprisingly found that HOS1 proteins could barely be detected in the *nup96-1* background, and this loss of HOS1 proteins was restored in the *Nup96-GFP nup96-1* complementation line (Figure 5B).

We then performed a detailed comparison of the HOS1 protein levels between the wild type and *nup96-1* mutants in a time-of-day manner. As expected, HOS1 proteins were undetectable at all time points in the *nup96-1* mutant (Figure 5C), although the overall level of *HOS1* mRNA was slightly higher in the *nup96-1* mutant than in wild-type plants (Figure 5A). This observation was confirmed by two other experiments. First, we created transgenic plants expressing the *HOS1-GFP* fusion gene driven by the *HOS1* native promoter (including the 5′ untranslated region of *HOS1*) in wild-type plants (*HOS1*$_{pro}$:*HOS1-GFP* wild type) and introduced this transgene into the *nup96-1* background by genetic cross. HOS1-GFP proteins could be microscopically visualized in wild-type plants but not in *nup96-1* mutants (Figure 5D). Second, we expressed the *HOS1-myc* coding sequence under the control of the 35S promoter in the wild-type background (*35S*:*HOS1myc* wild type), and two such lines (no. 1 and no. 2) were selected to cross with *nup96-1* mutants. Then, we compared HOS1-myc protein levels in the wild type with those of *nup96-1* mutants at two time points (ZT4 and ZT16) by immunoblot assays. The results showed that HOS1-myc proteins were completely destroyed in *nup96-1* mutants (Figure 5E).

To further investigate the relationship between Nup96 and HOS1, we performed an in vitro assay (Ruan et al., 2019) to detect the effect of Nup96 on the stability of HOS1 proteins by incubating purified recombinant His-HOS1 proteins with tissue extracts from the *nup96-1* mutant and wild-type plants. Not surprisingly, the recombinant HOS1 proteins were much more sensitive to the seedling extract of the *nup96-1* mutant, compared with the seedling extract of wild-type Col-0, and degraded much quickly (Figures 5F and 5G).

Thus, all the evidence above strongly suggests that Nup96 is required for stabilizing HOS1 proteins in Arabidopsis. However, we could not rule out the possibility that translation inefficiency is also a contributing factor for the deaccumulation of HOS1 proteins in *nup96* mutants. This unexpected finding prompted us to examine whether HOS1 had a similar effect on Nup96 protein stability. In an immunoblot assay using anti-Nup96 antibodies, the endogenous Nup96 level was reduced in *hos1-3* mutants (Figure 5H), but with unchanged *Nup96* mRNA abundance (Figure 5I). Together, these results suggested a mechanism of mutual stabilization of HOS1 and Nup96 proteins in plants.

Nup96 and *HOS1* Overlappingly Regulate Flowering Time in Plants

The above results showed that *Nup96* and *HOS1* may have overlapping functions in flowering regulation in Arabidopsis. To test this hypothesis using genetic and molecular approaches, we first constructed the *nup96-1 hos1-3* double mutant by crossing. While *nup96-1* mutants recapitulated the early-flowering phenotype of plants defective in *HOS1* function (*hos1-3*), the *nup96-1 hos1-3* double mutant did not display a much earlier flowering phenotype than either of its parental lines in both long days and short days (Figures 6A and 6B), suggesting that a similar molecular mechanism might be shared by both single and double mutants in photoperiodic flowering.

To further investigate the functional relationship of *Nup96* and *HOS1* genes in flowering control in plants, we performed RNA sequencing (RNA-seq) to interrogate the transcriptomic changes caused by *Nup96* or *HOS1* mutation. In comparison with wild-type plants, 2204 and 1924 genes were differentially expressed in the *nup96-1* and *hos1-3* mutants (Supplemental Data Set 2), respectively, whose expression levels showed a clear positive correlation (Pearson correlation coefficient = 0.884; $P < 2.2 \times 10^{-16}$; Figure 6C). Moreover, >50% of either downregulated or upregulated genes in *nup96-1* and *hos1-3* mutants were overlapping (Figures 6D and 6E). We also found that, consistent with the phenotypic observations, many flowering-related genes were misregulated in both mutants (Figure 6F). Overall, most of the differentially expressed floral promoting genes, including *FT*, *GA2ox2*, and *SOC1*, were upregulated, whereas the floral repressing genes, such as *miR156*, *CCA1*, and *RVE*, were downregulated, indicating that various flowering time genes may contribute to the early flowering of both *nup96* and *hos1* mutants. These results are in strong agreement with the notion that Nup96 and HOS1 partially share a common mechanism in flowering regulation in Arabidopsis.

Gene Ontology (GO) analyses revealed that the top 20 significantly enriched terms (ranked by $P < 0.01$) of down-regulated genes in both mutants are almost defense response-related (Supplemental Figures 3A and 3C), while the upregulated genes elicited by two gene mutations were shown to respond to various abiotic environmental stimuli, phytohormones, and chemical compounds (Supplemental Figures 3B and 3D), in agreement with previous observations (Zhang and Li, 2005; Dong et al., 2006; Parry et al., 2006; Lee et al., 2012; Parry, 2014; Lazaro et al., 2015; Lee and Seo, 2015; MacGregor and Penfield, 2015).

In summary, our data demonstrate that Nup96 and HOS1 are mutually stabilized and have overlapping functions not only in flowering regulation but also in other multiple physiological processes.

Loss of *Nup96* Functions Strikingly Promotes CO Accumulation

HOS1, functioning as an E3 ubiquitin ligase, is involved in the proteasome-dependent degradation of CO proteins in response to different environmental factors (Jung et al., 2012; Lazaro et al., 2012, 2015). Therefore, we reasoned that if HOS1 was inactivated in *nup96* mutants, then CO proteins would overaccumulate in this background, which might lead to early flowering. To test this hypothesis, we introduced the *HA-CO* transgene into the *nup96-1* background by crossing the *nup96-1* mutant with the *CO*$_{pro}$:*HA-CO co-10* line (Sarid-Krebs et al., 2015). In both the nuclear (Figures 7A–7D) and the whole (Supplemental Figure 4) protein extracts from plants grown in long days, CO proteins indeed exhibited higher levels in *nup96-1* mutants than in the wild type (Columbia [Col]), specifically from dusk to the early morning. Consistent with the high abundance of CO proteins, *FT* was expressed at high levels in the late part of this phase (Figure 7E), suggesting that the early-flowering phenotype of the *nup96-1* mutant was the result of the accumulation of CO proteins in the morning. However, the *CO* transcript level was

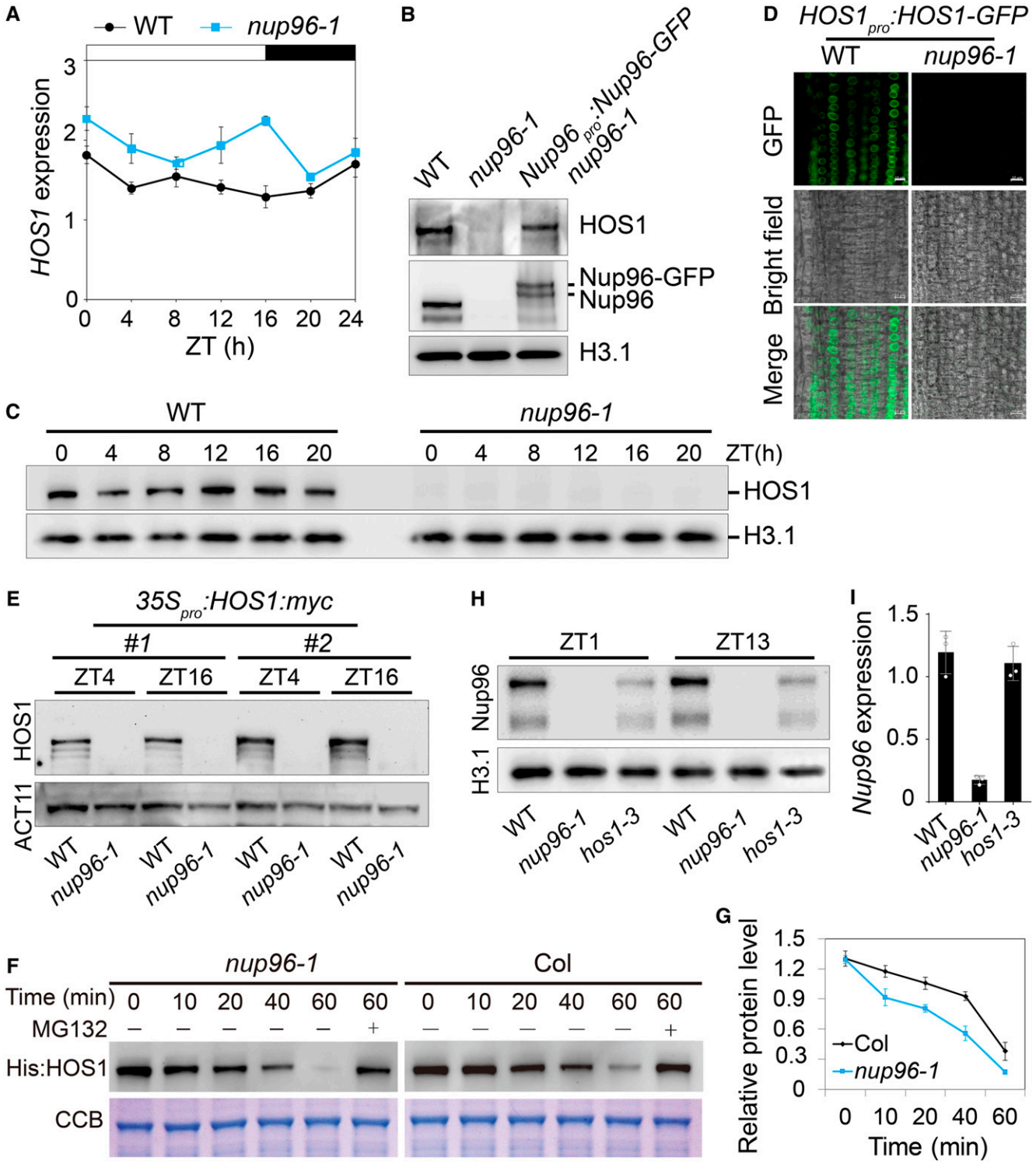

Figure 5. Nup96 Stabilizes HOS1 Proteins in Plants.

(A) Diurnal expression of *HOS1* in wild-type (WT) and *nup96-1* seedlings grown in long-day conditions for 9 d. Values are means ± SD ($n = 3$ biological repeats).

(B) Immunoblot shows HOS1 levels in the nuclear extracts from the WT, *nup96-1*, and *Nup96-GFP nup96-1* complementation plants. Histone H3.1 (H3.1) was used as the loading control.

not noticeably altered by *nup96* mutation (Figure 7F). To determine whether the overaccumulated CO proteins were responsible for the early flowering of *nup96* plants, we generated the *nup96-1 co-9* double mutant and observed that the flowering time of *nup96-1* mutants grown in long days was significantly delayed by the *co* mutation (Figures 7G and 7H). However, in short days, the *nup96-1 co-9* double mutant flowered as early as the *nup96-1* single mutant (i.e., not having the later-flowering character of the *co-9* mutant), reminiscent of the effect of *co-2* on *hos1-2* in flowering regulation (Lazaro et al., 2012), where the flowering time of *hos1-2 co-2* is similar to that of the *hos1-2* mutant but not to that of the *co-2* mutant. Such a phenotype supported the hypothesis that *Nup96* and *HOS1* are involved in the regulation of flowering in a similar *CO*-dependent pathway in long-day conditions but not in short-day conditions, because *CO* is confirmed to be an activator of Arabidopsis flowering only in long days but not in short days (Rédei, 1962; An et al., 2004; Datta et al., 2006). Furthermore, *FT* and *SOC1* expression in *nup96-1 co-9* double mutants was as low as that in *co-9* mutants (Figure 7I). These data strongly suggested that *CO* acts genetically downstream of *Nup96* and *HOS1*, and the early flowering of *nup96* mutants could be largely attributed by the increased CO protein level. Therefore, the results revealed a novel repression mechanism of flowering, where Nup96 and HOS1 proteins were mutually stabilized to control CO protein homeostasis to gate flowering and loss of one of them (Nup96 or HOS1) led to degradation of the other proteins conferring early flowering in Arabidopsis (Figure 8).

DISCUSSION

As plants live in temporally fluctuating environments, the negative regulatory mechanisms that prevent precocious flowering are critical. Here, we present a set of data that elucidates the involvement of nucleoporin Nup96 in flowering regulation in Arabidopsis. Autocleavage of Nup96 proteins is conserved in all eukaryotes (Fontoura et al., 1999; Iwamoto et al., 2010), but it is not necessary for both the subcellular localization and flowering activity of Arabidopsis Nup96 proteins (Figure 2), suggesting that the significance of autocleavage of Nup96 proteins in plants remains to be uncovered. We further reveal a novel floral repression mechanism in Arabidopsis, where a nuclear pore complex component, Nup96, interacts with and stabilizes a floral repressor, HOS1, to balance the activity of flowering promotion pathways, allowing plants to eventually flower at the most advantageous time (Figure 8).

It has been reported that *hos1* mutants exhibit early-flowering phenotypes under various light and temperature regimes (Ishitani et al., 1998; Jung et al., 2012; Lazaro et al., 2012; Lee et al., 2012). Very much like *hos1* mutants, *Nup96* mutation also causes early flowering under both long days and short days, with quite similar leaf numbers to that of *hos1-3* mutants (Figures 1B and 1E). Moreover, no additive effect was observed when comparing the flowering time of the *nup96-1 hos1-3* double mutant with either of its parental lines (Figures 6A and 6B). Molecular mechanisms of HOS1-dependent flowering repression have been well studied recently (Jung et al., 2012, 2013; Lazaro et al., 2012, 2015), one of which involves HOS1-mediated CO protein degradation. Under long days, the flowering time of the *hos1* mutant could be strongly suppressed by *CO* mutation, but under short days, *hos1 co* double mutants flower as early as *hos1* (Lazaro et al., 2012), suggesting that HOS1 regulates flowering time through a CO-dependent mechanism in long days but a CO-independent mechanism in short days. A similar observation was made in *nup96 co* double mutants (Figures 7G and 7H). As observed in *hos1*, increased CO abundance was seen in *nup96* mutants, but with slightly different patterns (Figures 7A–7D; Supplemental Figure 4). In long day-grown *nup96-1*, CO accumulated from dusk to the early morning and resulted in the activation of *FT* in this phase to trigger flowering, whereas CO showed higher levels in *hos1* plants in the day but not in the evening (Jung et al., 2012; Lazaro et al., 2012). One possible explanation for this discrepancy might be that Nup96 modulates CO degradation not only through HOS1 but also through another E3 ligase of CO, such as COP1, which functions late in the day (Jang et al., 2008; Liu et al., 2008; Sarid-Krebs et al., 2015). Therefore, more studies might be needed to test if COP1 activity is compromised in *nup96* mutants. In summary, the evidence strongly suggests that *Nup96* and *HOS1* might regulate photoperiodic flowering through similar mechanisms. In addition, our data from RNA-seq (Figure 6) clearly demonstrate that many other genes, such as *GA2ox2*, *SOC1*, *miR156*, *CCA1*, and *RVE*, may function in the regulation of the *nup96* and *hos1* early-flowering phenotype. Therefore, *CO* may not be the only regulator of flowering in the *nup96* and *hos1* mutants in long days. In addition to early flowering, *HOS1*-deficient plants also show a lengthened period of circadian clock (MacGregor et al., 2013). It would be particularly interesting to investigate if *Nup96* is also

Figure 5. (continued).

(C) Levels of endogenous HOS1 proteins in the nuclear extracts from WT and *nup96-1* seedlings grown in long-day conditions for 9 d, detected by anti-HOS1 antibodies. Histone 3.1 was used as the loading control.

(D) HOS1-GFP signals in wild-type and *nup96-1* seedling root cells. Bars = 10 μm.

(E) Levels of HOS1-myc proteins in the nuclear extracts from WT and *nup96-1* seedlings grown in long-day conditions for 9 d. ACTIN11 (ACT11) was used as the loading control.

(F) Assay of HOS1 protein stability in vitro. His:HOS1 proteins were purified from *Escherichia coli* and incubated with the total extracts of *nup96-1* or Col-0 seedlings in the presence or absence of MG132. His:HOS1 proteins were probed by His antibody on an immunoblot (upper panel). Coomassie Brilliant Blue (CBB) staining is shown in the lower panel.

(G) Quantitative assay of HOS1 protein levels from three biological repeats with a representative result shown in **(F)**.

(H) Levels of endogenous Nup96 proteins in the nuclear extracts from WT, *hos1-3*, and *nup96-1* seedlings grown in long-day conditions for 9 d.

(I) qPCR analysis of *Nup96* expression in WT, *hos1-3*, and *nup96-1* seedlings grown in long-day conditions for 9 d. Values are means ± SD ($n = 3$ biological repeats).

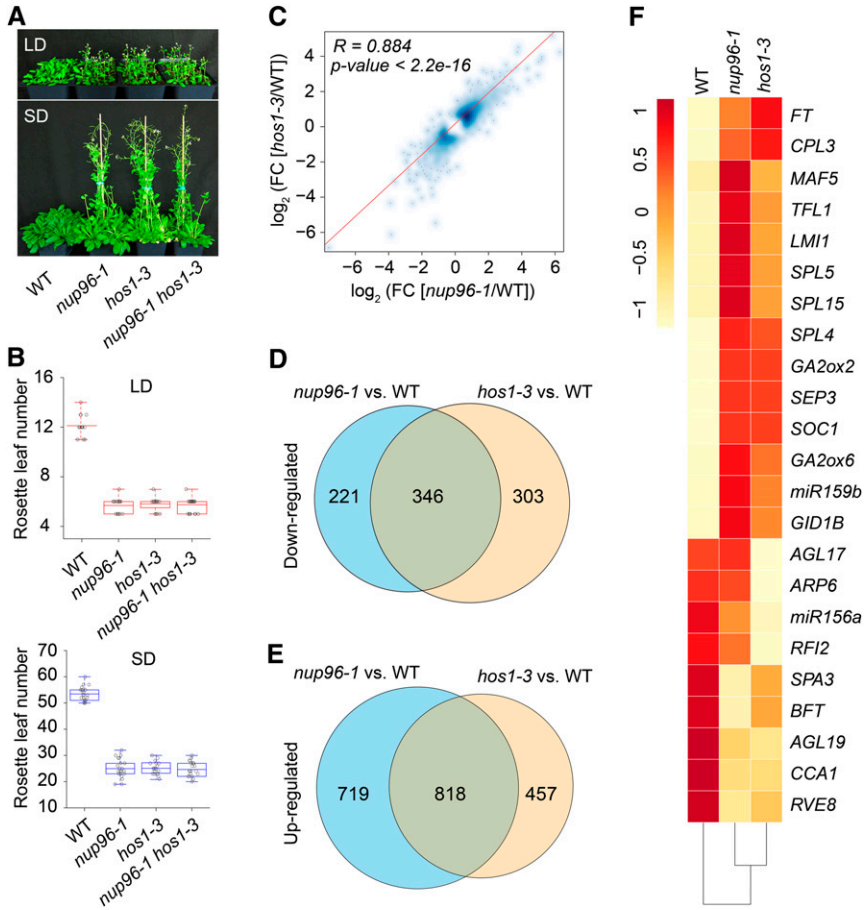

Figure 6. *Nup96* and *HOS1* Mutations Cause Similar Transcriptomic Changes in Plants.

(A) Flowering phenotypes of the wild type (WT), *nup96-1* and *hos1-3* single mutants, and *nup96-1 hos1-3* double mutants grown in long days (LD) and short days (SD).

(B) Rosette leaf numbers at the time of flowering for the genotypes shown in **(A)**; $n > 20$. Box plots are used to display the distributions of data points (presented as circles). The lines in the box (from top to bottom) indicate the maximum, third quartile, mean, first quartile, and minimum. Red boxes and blue boxes present the data in long days and short days, respectively. WT, wild type.

(C) Scatterplot showing the expression correlation of differentially expressed genes in *nup96-1* and *hos1-3* mutants compared with the WT. Differentially expressed genes from RNA-seq data are defined as those with a fold change (FC; mutant/wild type) > 1.5 or < 0.67 (Fisher's exact test, $P < 0.01$ and FDR < 0.01; Supplemental Data Set 2). The red line is the linear regression. *R*, Pearson correlation coefficient.

(D) and **(E)** Venn diagrams depicting the overlaps between the downregulated genes **(D)** and the upregulated genes **(E)** in *nup96-1* and *hos1-3* mutants. WT, wild type.

(F) Heatmap presenting the misregulated flowering time genes in *nup96-1* or *hos1-3* mutants compared with WT.

required for maintaining the normal circadian clock periodicity and if the altered circadian clock function in *hos1* contributes to its early-flowering phenotype.

A previous study by Tamura et al. (2010) shows that conserved components of the nuclear pore complex, RNA EXPORT FACTOR1 (RAE1) and Nup43, are able to interact with HOS1 in plants, suggesting an association of HOS1 with the nuclear pore complex. In our study, by using Nup96 as the bait, we found that Nup96 interacted with HOS1 at the nuclear envelope in vivo (Figure 5D). Therefore, Nup96 is only one of several HOS1-interacting proteins and may serve as one of the docking sites of HOS1 proteins on the nuclear membrane. Interestingly, RAE1, Nup43, and Nup96 are all located at the outer ring of the nuclear pore. Nup43 and Nup96 are components of the Nup107-160 subcomplex (Boruc et al., 2012; González-Aguilera and Askjaer, 2012), while RAE1 has been reported to stably associate with Nup98 and the mRNA export factor TAP in *Xenopus laevis* egg extracts (Blevins et al., 2003). Interactions of HOS1 with diverse proteins of the nuclear pore complex might suggest that nuclear pore targeting of HOS1 is linked to its multiple molecular activities via dependent or independent mechanisms. Other studies also reveal that HOS1 interacts with ICE1, CO, FVE, and HDA6 in the nucleus (Dong et al., 2006; Jung et al., 2012, 2013; Lazaro et al., 2012), indicating that HOS1 might dynamically shuttle between the nuclear pore and nucleoplasm. It would be interesting to investigate how and when Nup96 interacts with HOS1 proteins and to determine their

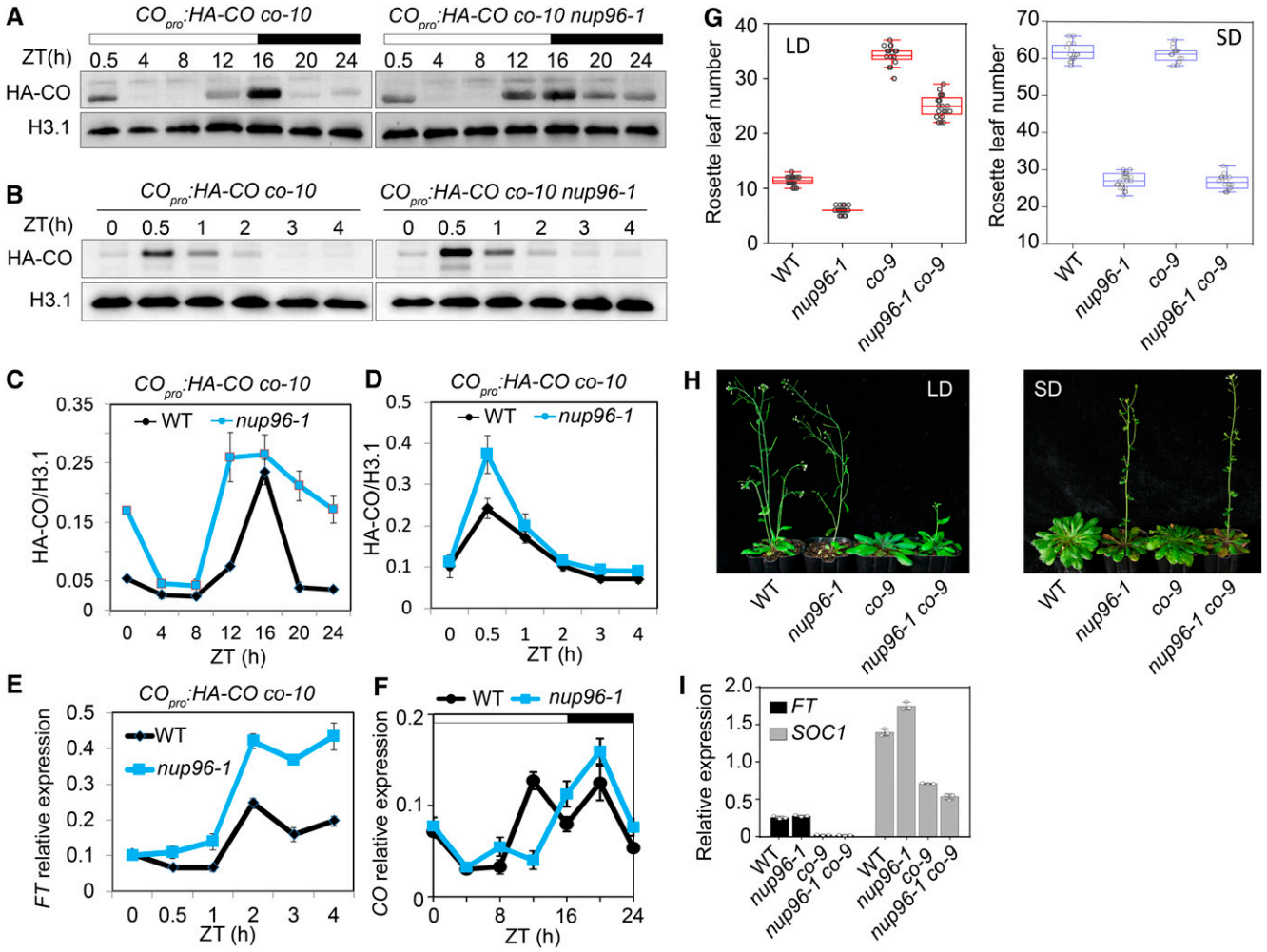

Figure 7. Loss of *Nup96* Function Promotes CO Accumulation, Resulting in an Early-Flowering Phenotype in Long Days.

(A) and **(B)** CO protein levels in nuclear extracts from the indicated transgenic plants (*CO*$_{pro}$*:HA-CO co-10* versus *CO*$_{pro}$*:HA-CO co-10 nup96-1*). Histone H3.1 (H3.1) was used as the loading control.

(C) and **(D)** Quantification of CO levels in immunoblots of **(A)** and **(B)**, respectively. Values are means ± SE ($n = 3$ biological repeats). WT, wild type.

(E) Expression levels of *FT* in the morning phase as in **(B)** and **(D)** in *CO*$_{pro}$*:HA-CO co-10* versus *CO*$_{pro}$*:HA-CO co-10 nup96-1* in long-day conditions for 9 d. Values are means ± SE ($n = 3$ biological repeats). *IPP2* (At3g02780) was used as a reference gene. WT, wild type.

(F) Diurnal expression of *CO* in the wild type (WT) and *nup96-1* mutants grown in long-day conditions for 9 d. Values are means ± SE ($n = 3$ biological repeats). *TIP41* (At4g34270) was employed as a control gene.

(G) Rosette leaf numbers at the time of flowering for the genotypes of WT, *nup96-1* and *co-9* single mutants, and *nup96-1 co-9* double mutants in long-day (LD) and short-day (SD) conditions ($n > 20$). Box plots are used to display the distributions of data points (presented as circles). The lines in the box (from top to bottom) indicate the maximum, third quartile, mean, first quartile, and minimum.

(H) Flowering phenotypes of WT, *nup96-1* and *co-9* single mutants, and *nup96-1 co-9* double mutants grown in long days (left) and short days (right).

(I) Expression analysis of *FT* and *SOC1* in different genotypes indicated in **(H)**. Values are means ± SD ($n = 3$ biological repeats). WT, wild type.

functions in the nucleoplasm and how HOS1 shuttles between the nuclear pore complex and nucleoplasm. However, the precise molecular functions of the Nup96-HOS1 module are not fully understood. The only evidence linking the activities of Nup96 and HOS1 at the molecular level is that both proteins play essential roles in mRNA nuclear export (Parry et al., 2006; MacGregor et al., 2013). In this regard, it is reasonable to infer that Nup96 and HOS1 work in concert to regulate mRNA nuclear export. However, the exact biological relevance of this molecular activity remains unclear. Another key aspect of HOS1 function is to modulate gene expression either through degrading transcription factors or interacting with transcription regulators. An additional study also demonstrates the association of HOS1 with chromatin in plants (Jung et al., 2013). Moreover, an interesting finding is showcased in the recent work that nonrandom regions on the chromosome are anchored at the nuclear periphery in Arabidopsis (Bi et al., 2017). Our evidence shows that HOS1 and Nup96 regulate the expression of an overlapping set of genes (Figure 6). Based on

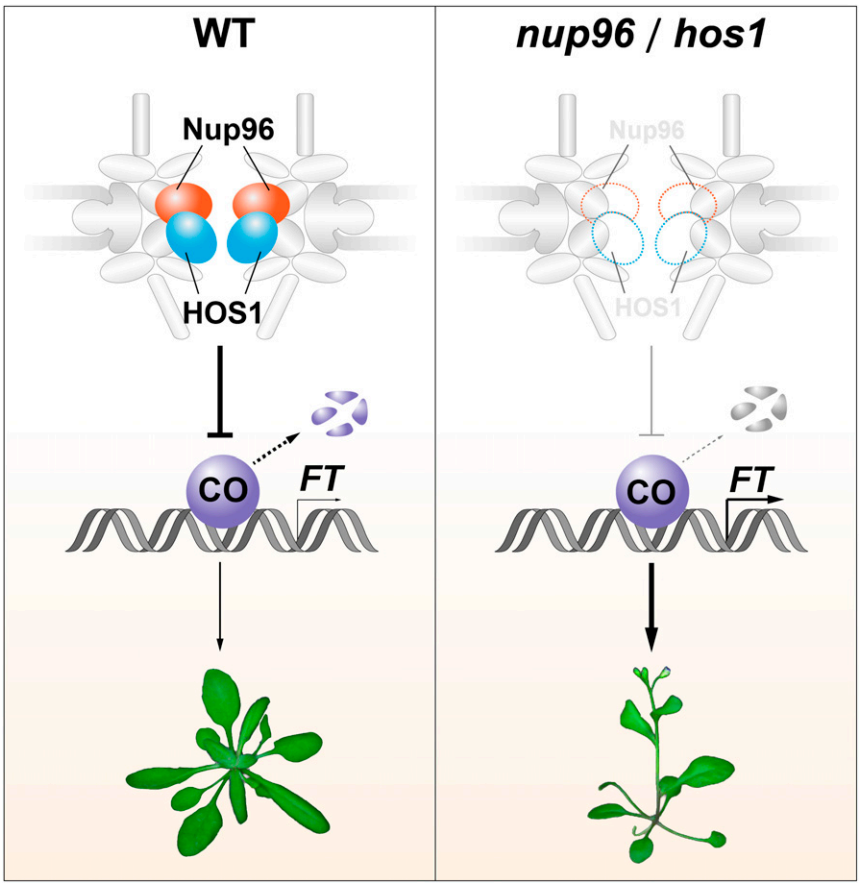

Figure 8. Model Depicting the Molecular Mechanism of Nup96/HOS1-Mediated Flowering Regulation.

In the wild type (left), Nup96 mutually associates with and stabilizes the floral repressor HOS1 to facilitate the degradation of CO proteins, preventing precocious flowering. Loss of either *Nup96* or *HOS1* function (right) results in the destruction of HOS1 or Nup96 proteins, leading to overaccumulation of CO proteins in plants. The elevated CO abundance enhances *FT* expression, causing early flowering. WT, wild type.

these lines of evidence, it would be interesting to establish if Nup96-HOS1 have the capability to anchor the chromosome at the nuclear periphery and thereby exert their influence on gene transcription activities.

The interaction of Nup96 and HOS1 not only links the activities of both genes but also leads to an unexpected mutual stabilization of the two proteins (Figure 5). Our results revealed that the *nup96* mutation resulted in the destruction of endogenous HOS1 proteins (Figures 5C, 5E, and 5F). In *hos1* plants, the Nup96 protein level was significantly reduced (Figure 5H), suggesting that HOS1 is directly or indirectly important for Nup96 protein turnover. Strikingly, we noticed that the decrease of HOS1 in *nup96-1* was much more severe than that of Nup96 in *hos1-3*, suggesting that Nup96 is more important for HOS1 stability than vice versa and that some other factors may be involved in regulating Nup96 protein stability. However, how both proteins are degraded is still unknown. The similar mutual stabilization mechanism is also found in the ZTL-GI protein pair for maintaining the robustness of the circadian system in plants (Kim et al., 2007). The Nup96-HOS1 complex may limit the CO protein level to below a certain threshold in unfavorable conditions or at various developmental stages. For example, at early developmental stages, if CO proteins reach the threshold, plants would go into reproductive growth (early flowering) and produce a limited number of seeds due to limited vegetative growth, as was observed in mutant lines with an early-flowering phenotype, such as *nup96* and *hos1* mutants, so that it would be challenging for a species to survive. In this case, it would be interesting to determine how the activity of Nup96 and HOS1 is finely controlled.

Our findings define a novel regulatory mechanism that adds more complexity to the posttranscriptional processes that contribute to flowering time control in Arabidopsis. Interestingly, Arabidopsis plants deficient in another component of the Nup107-160 complex, Nup160 (also known as SAR1), have a similar early-flowering phenotype to that of *nup96* and *hos1* (Parry et al., 2006; Parry, 2014), suggesting the need to investigate if HOS1 proteins are diminished in the *nup160* background. Given that most components of the nuclear pore complex are conserved among plants and animals, it would also be interesting to test if the mutual stabilization mechanism of Nup96-HOS1 is conserved among their counterparts in different evolutionary lineages. As several nucleoporins can interact with HOS1, future work should examine

the specificity between HOS1 and different nucleoporins, crosstalk among these protein interactions, and their contributions to different cellular processes.

METHODS

Plant Materials and Growth Conditions

All Arabidopsis (*Arabidopsis thaliana*) lines used in this work are of the Col accession. *nup96-1* (SALK_109959), *nup96-2* (SALK_117966), *hos1-3* (SALK_069312), and *co-9* (SAIL_24_H04) were obtained from the ABRC (Ohio State University). Other mutants were described previously: *ft-1* (Yoo et al., 2005), *soc1-2* (Lee et al., 2000), and *co-10* (Laubinger et al., 2006). Seeds were placed on a moist filter paper and stratified at 4°C for 2 d, then transferred to soil and grown in either long-day (16 h of light/8 h of dark) or short-day (8 h of light/16 h of dark) conditions at 22°C. GreenPower LED toplighting (Philips Horticulture LED), with an intensity of 250 μmol m^{-2} s^{-1}, was used. For measuring flowering time, the numbers of rosette and cauline leaves were counted when plants were bolting. More than 20 plants were counted and averaged for each measurement.

Nup96 Antibody Preparation and Verification by IP

The peptide (amino acid residues from 505 to 959) of Nup96 protein was used as the antigen to develop Nup96-specific antibody by Abmart. To verify the specificity of Nup96 antibody, 12-d-old seedlings of Col-0, *nup96-1*, and *nup96-2* were collected and ground to fine powder in liquid nitrogen. Three volumes of extraction buffer (20 mM Tris-HCl, pH 7.4, 150 mM NaCl, 1% Triton X-100, 0.5 mM EDTA, 1 mM phenylmethylsulfonyl fluoride (PMSF), 1 mM DTT, and 1× protease inhibitor mixture [Roche]) was added to the sample. After homogenization on ice for 20 min, the mixture was centrifuged at 13,000*g* at 4°C for 10 min. The supernatant was transferred to a new tube, 10% of which was saved as "input" sample. IP was performed as follows: 5 μL of Nup96 antibody was added to the cleared protein extracts. After incubation at 4°C for 3 h, 30 μL of Protein A/G-agarose (Abmart, A10001) was added and incubated for another 2 h at 4°C. After washing Protein A/G-agarose with extraction buffer (without protease inhibitor cocktail) five times, the proteins were eluted with 2× SDS-PAGE loading buffer by heating at 95°C for 5 min and separated on a 4 to 20% SurePAGE precast gel (Genscript, M00657) followed by immunoblot analyses.

nup96 Complementation and Autocleavage Site Analyses

The 2.5-kb region upstream of the ATG start codon was used as the promoter sequence of *Nup96*, which was inserted into the Fu76 entry vector (Wang et al., 2013). To identify the autocleavage of *Nup96*, the different versions of *Nup96* (*Nup96*, *Nup96* $\triangle N$ [a deletion mutant of 187 amino acids of the N-terminal end], and *Nup96m* [two point mutations, F187Q and S188A]) were cloned into the Fu28 entry vector (Wang et al., 2013). The 2.5-kb promoters and these versions of *Nup96* sequences were integrated into the Fu39-2 destination vector (Wang et al., 2013) by LR Clonase (Invitrogen, 11791020). The resulting binary vectors were transformed into the *nup96-1* mutant, respectively. The 12-d-old seedlings were used for analyzing autocleavage sites by immunoblot assays. The 2-d-old seedlings were used for examining protein subcellular localizations under an LSM 710 microscope (Carl Zeiss). Propidium iodide (20 μg/mL) was used for cell wall staining.

Protein Complex Identification by LC-MS/MS

The *$Nup96_{pro}$:Nup96-GFP nup96-1* and *35S:GFP* wild-type seedlings were grown in long-day conditions for 12 d, and two replicate samples (~4 g for each sample) for each genotype were harvested. The seedlings were pooled and frozen in liquid N_2 at ZT4 for protein extraction. GFP-trap agarose beads were used for IP of Nup96-GFP and GFP protein complexes as described previously (Wang et al., 2015). After elution from the beads, the IP samples were subjected to LC-MS/MS analysis (Shanghai Applied Protein Technology).

Gene Expression Analysis

For gene expression analyses, 12-d-old seedlings grown on MS medium supplemented with 3% sucrose and 0.6% agar were collected for RNA extraction with an EasyPure Plant RNA Kit (Transgen Biotech, ER301-01). Total RNA concentration was measured by Nanodrop 2000 (Thermo Fisher Scientific NanoDrop). Total RNA (1 μg) was used for first-strand cDNA synthesis using FastKing genomic DNA Dispelling RT SuperMix (Tiangen, KR170801). qPCR analyses were performed with SYBR Premix Ex Taq (TaKaRa) on a StepOne Plus Realtime PCR system (Applied Biosystems) as described previously (Marshall et al., 2016). To detect the full-length transcripts of *Nup96* in both wild-type plants and *nup96* mutants, regular RT-PCR was performed using cDNA described above as the template. *ACTIN* was used as the internal control in RT-PCR, while either *IPP2* or *PP2A* was used as the internal control for qPCR. All sequences of primers are listed in the Supplemental Table.

GUS Staining

Seedlings were soaked in GUS staining solution (50 mM sodium phosphate, pH 7.2, 0.5 mM potassium ferricyanide, 0.5 mM potassium ferrocyanide, 20% [v/v] methyl alcohol, and 2 mM 5-bromo-4-chloro-3-indolyl-β-D-glucuronic acid, cyclohexylammonium salt] and subjected to a vacuum for 15 min, then incubated at 37°C for 16 to 20 h in the dark. After incubation, chlorophyll was removed from seedlings by washing in the destaining buffer (75% [v/v] ethanol and 25% [v/v] acetic acid) three to five times. The seedlings were observed using a stereomicroscope with a SZ2-ILST CCD camera (Olympus).

BiFC

HOS1 full-length coding sequence and *cYFP* were cloned into Fu66 (Wang et al., 2013) to generate Fu66-*HOS1-cYFP*, which was cloned into Fu39-*2-35S* by the LR reaction to generate Fu39-*2-35S:HOS1-cYFP* binary vector. *Nup96* full-length coding sequence and *nYFP* were cloned into Fu66 (Wang et al., 2013) as well to generate Fu66-*Nup96-nYFP*, which was cloned into Fu39-2-*35S* by the LR reaction to generate Fu39-2-*35S:Nup96-nYFP* binary vector. Fu39-2-*35S:Nup96-nYFP* and Fu39-2-*35S:HOS1-cYFP* were transformed into Col-0 separately. The two resulting transgenic lines were crossed to generate plants coexpressing *35S:Nup96:nYFP* and *35S:cYFP:HOS1*, which were used to detect the signal of reconstituted YFP fluorescence by laser scanning confocal microscopy (LSM 710, Carl Zeiss).

Co-IP

For co-IP analyses, *pGWC-HOS1* was integrated into *pGWB20* (Tanaka et al., 2012) to obtain *pGWB20-35S:HOS1-myc*, which was used to transform wild-type Arabidopsis. *$Nup96_{pro}$:Nup96:GFP nup96-1* and *35S:HOS1-myc* wild type were crossed to generate a transgenic line expressing both *$Nup96_{pro}$:Nup96:GFP* and *35S:HOS1-myc*. Protein extraction and IP were performed as described for LC-MS/MS analyses. For the immunoblot assay, anti-GFP antibody (MBL, 598) and anti-myc antibody (Abmart, M20002) were used to detect Nup96-GFP and HOS1-myc, respectively. Anti-HSP90 antibody (Sigma-Aldrich, SAB1305541) was used to detect endogenous HSP90 proteins as the loading control.

HOS1 Protein Analysis

To generate the *HOS1$_{pro}$:HOS1-GFP* construct, the 2.78-kb genomic sequence upstream of the start codon was cloned into pFu76 (Wang et al., 2013) as the *HOS1* promoter entry clone. Full-length *HOS1* coding sequence was cloned into pFu28 (Wang et al., 2013) to produce the *HOS1-GFP* gene entry clone. These two plasmids were integrated into the pFu39-2 destination vector (Wang et al., 2013) to generate the *HOS1$_{pro}$:HOS1-GFP* binary vector, which was transformed into Col-0. Then, *HOS1$_{pro}$:HOS1-GFP* wild type was introduced into *nup96-1* mutants by genetic cross. The *HOS1$_{pro}$:HOS1:GFP nup96-1* homozygous line was used to analyze HOS1 protein stability. To examine the colocalization of HOS1 and Nup96 proteins, we generated transgenic lines separately expressing *gHOS1:mCherry* and *gNup96:GFP* transgenes (*gHOS1* and *gNup96* denote genomic DNA of *HOS1* and *Nup96*, respectively, including promoter sequences and coding sequences). Then, two single transgenic lines were crossed to generate the plants coexpressing *gHOS1:mCherry* and *gNup96:GFP*. *gHOS1:mCherry* and *gNup96-GFP* single and dual transgenic lines were used to observe the protein subcellular localizations by laser scanning confocal microscopy (LSM 710, Carl Zeiss).

In Vitro Stability Assay for HOS1 Proteins

The 12-d-old seedlings of the *nup96-1* mutant and wild-type Col-0 grown in long days were harvested at ZT4 for total protein extraction with Tris-HCl extraction buffer (25 mM Tris-HCl, pH 7.5, 10 mM NaCl, 10 mM $MgCl_2$, 4 mM PMSF, 5 mM DTT, and 10 mM ATP) according to a previous report (Ruan et al., 2019). The coding sequence of HOS1 was cloned into pET28a with *Bam*HI and *Sal*I, and the resulting vector was transformed into *Escherichia coli* BL21(DE3) for recombination protein expression. The His:HOS1 proteins was purified by Ni-NTA agarose (Qiagen, 30230). The reaction for stability assay was set up by mixing His-HOS1 proteins (100 ng) and seedling extracts (400 μg of proteins) with or without MG132 (a final concentration of 50 μM). The reaction was stopped in time by adding SDS-loading buffer and subjected to immunoblot analysis, which was probed by His antibody (Abmart, M20020) for detecting His-HOS1 proteins. Coomassie Brilliant Blue staining was applied to show the amount of loading proteins. At least three independent biological repeats were performed.

Analysis of HA-CO Protein Abundance in Vivo

Seedlings grown under long-day conditions for 12 d were harvested and ground to fine powder in liquid nitrogen. Nuclear proteins were extracted as previously described (Hayama et al., 2017). Briefly, ~500 μL of powder was mixed with 1 mL of nuclear extraction buffer (20 mM Tris-HCl, pH 6.8, 20 mM $MgCl_2$, 5% sucrose, 40% glycerol, 0.3% Triton X-100, 0.08% β-mercaptoethanol, 0.2% plant protease inhibitor, 1 mM DTT, and 1.3 mM PMSF). The samples were then centrifuged at 3800*g* for 5 min at 4°C. The pellet was washed with nuclear extraction buffer three to four times until it became colorless. The pellet was heated at 95°C for 10 min in 2× SDS-PAGE loading buffer and then loaded on a precast gel (8% SurePAGE precast gel, M00663, Genscript). Anti-HA antibody (Roche, 11867423001) was used to detect HA-CO proteins. Anti-histone H3.1 (Abmart, P30266) and anti-ACT11 (Abmart, M2009) antibodies were used as loading controls. Signals on blots were quantified using ImageJ software.

RNA-Seq and Data Analysis

For the RNA-seq experiment, seedlings grown in long-day conditions for 12 d were harvested at ZT15, pooled for each genotype, frozen in liquid N_2, and stocked at −80°C. The samples were ground in liquid N_2 and then divided into three parts for each genotype (considered as three repeats). The three repeats of each sample were subjected to RNA isolation and library construction independently. Total RNAs were prepared as described above, and the quality of RNA samples was analyzed with a 2100 Bioanalyzer (Agilent). Barcoded cDNA libraries were constructed using Illumina Poly-A Purification TruSeq library reagents and protocols. Samples of three biological repeats were sequenced on Illumina HiSeq 2500 V4 (paired-end 125-bp run). The paired-end reads were aligned to the Arabidopsis genome (TAIR10) using tophat-2.0.11 with an anchor length of more than eight nucleotides for spliced alignments. Only the reads that were uniquely aligned were retained for subsequent analyses. The relative abundance of mRNA was normalized and presented as fragments per kilobase of transcript per million mapped reads. The P value and false discovery rate (FDR) were calculated using the edgeR package of Bioconductor. Genes that showed larger than 1.5-fold difference (fold change > 1.5) in the relative mRNA abundance with $P < 0.01$ and FDR < 0.01 were considered differentially expressed. GO enrichment calculation was performed with the gProfiler web server (https://biit.cs.ut.ee/gprofiler/gost). The top 20 most significantly enriched GO terms for each gene set were retrieved, and the $-\log_{10}$ P values were plotted by the heatmap function in R. RNA-seq data were submitted to the National Center for Biotechnology Information with Gene Expression Omnibus accession number GSE138706.

Phylogenetic Analysis

The amino acid sequences of 40 Nup96 proteins identified from 37 plant species were derived from Phytozome (https://phytozome.jgi.doe.gov/pz/portal.html; Supplemental Data Set 1). The sequences were aligned by the ClustalW program. An unrooted phylogenetic tree was then generated by the neighbor-joining method using MEGA 5 software. Bootstrap values shown at each branch were calculated from 1000 replicates.

Statistical Analysis

All experiments in this study were performed at least three times (i.e., three biological repeats), which means three experiments with independent pools of plants prepared at different times except for LC-MS/MS and RNA-seq, which are indicated in their own sections. All statistical analyses were performed using the SPSS software package, and representative data are shown. Asterisks indicate significant difference according to Student's *t* test (***, $P < 0.001$; **, $P < 0.01$; and *, $P < 0.05$). All results are summarized in Supplemental Data Set 3.

Accession Numbers

Accession numbers are as follows: *Nup96* (AT1G80680), *HOS1* (AT2G39810), *CO* (AT5G15840), *FT* (AT1G65480), *SOC1* (AT2G45660), *ACTIN* (AT5G09810), *IPP2* (AT3G02780), and *PP2A* (AT1G13320).

Supplemental Data

Supplemental Figure 1. Phylogenetic analysis of Nup96 proteins in green lineages.

Supplemental Figure 2. *Nup96* is broadly expressed and functions in diverse developmental processes in plants.

Supplemental Figure 3. *nup96* and *hos1* mutations have common transcriptomic changes in multiple pathways.

Supplemental Figure 4. CO proteins over-accumulate in *nup96* mutants.

Supplemental Table. List of primers used in this study.

Supplemental Data Set 1. Alignment used to generate the phylogeny presented in Supplemental Figure 1.

Supplemental Data Set 2. Differentially expressed genes identified using RNA-seq.

Supplemental Data Set 3. Statistical analysis in this study.

ACKNOWLEDGMENTS

We thank Ilha Lee (Seoul National University), Ji Hoon Ahn (Korea University), and the ABRC for kindly providing *soc1-2*, *ft-1*, and T-DNA insertion lines as well as George Coupland (Max Planck Institute for Plant Breeding) for kindly providing CO_{pro}:*HA*:*CO co-10* lines and *pLEELA* and *GW-MCS-NOS-pGREEN* vectors. We also thank Lianfeng Gu (Fujian Agriculture and Forestry University) for RNA-seq analysis and Meiqin Liu for technical assistance with confocal microscopy. This work was supported by the National Natural Science Foundation of China (grants 30670189 and 31370324).

AUTHOR CONTRIBUTIONS

Y.F. and X.W. conceived the project, designed the experiments, and analyzed the results; Z.C., X.Z., P.H., L.L., and G.H. designed and performed all the experiments and analyzed the results; J.Z., F.Z., and Y.M. helped to prepare *Nup96* overexpression and tissue-specific expression plants; Y.F., X.W., and Z.C. created all figures; Y.F., X.W., and L.L wrote the article.

Received August 29, 2019; revised October 17, 2019; accepted December 10, 2019; published December 11, 2019.

REFERENCES

Abe, M., Kobayashi, Y., Yamamoto, S., Daimon, Y., Yamaguchi, A., Ikeda, Y., Ichinoki, H., Notaguchi, M., Goto, K., and Araki, T. (2005). FD, a bZIP protein mediating signals from the floral pathway integrator FT at the shoot apex. Science **309:** 1052–1056.

An, H., Roussot, C., Suárez-López, P., Corbesier, L., Vincent, C., Piñeiro, M., Hepworth, S., Mouradov, A., Justin, S., Turnbull, C., and Coupland, G. (2004). CONSTANS acts in the phloem to regulate a systemic signal that induces photoperiodic flowering of Arabidopsis. Development **131:** 3615–3626.

Bi, X., Cheng, Y.J., Hu, B., Ma, X., Wu, R., Wang, J.W., and Liu, C. (2017). Nonrandom domain organization of the *Arabidopsis* genome at the nuclear periphery. Genome Res. **27:** 1162–1173.

Bilokapic, S., and Schwartz, T.U. (2013). Structural and functional studies of the 252 kDa nucleoporin ELYS reveal distinct roles for its three tethered domains. Structure **21:** 572–580.

Blevins, M.B., Smith, A.M., Phillips, E.M., and Powers, M.A. (2003). Complex formation among the RNA export proteins Nup98, Rae1/Gle2, and TAP. J. Biol. Chem. **278:** 20979–20988.

Boeglin, M., Fuglsang, A.T., Luu, D.T., Sentenac, H., Gaillard, I., and Chérel, I. (2016). Reduced expression of AtNUP62 nucleoporin gene affects auxin response in Arabidopsis. BMC Plant Biol. **16:** 2.

Boruc, J., Zhou, X., and Meier, I. (2012). Dynamics of the plant nuclear envelope and nuclear pore. Plant Physiol. **158:** 78–86.

Datta, S., Hettiarachchi, G.H.C.M., Deng, X.W., and Holm, M. (2006). Arabidopsis CONSTANS-LIKE3 is a positive regulator of red light signaling and root growth. Plant Cell **18:** 70–84.

de Montaigu, A., Tóth, R., and Coupland, G. (2010). Plant development goes like clockwork. Trends Genet. **26:** 296–306.

Dong, C.H., Agarwal, M., Zhang, Y., Xie, Q., and Zhu, J.K. (2006). The negative regulator of plant cold responses, HOS1, is a RING E3 ligase that mediates the ubiquitination and degradation of ICE1. Proc. Natl. Acad. Sci. USA **103:** 8281–8286.

Fontoura, B.M., Blobel, G., and Matunis, M.J. (1999). A conserved biogenesis pathway for nucleoporins: Proteolytic processing of a 186-kilodalton precursor generates Nup98 and the novel nucleoporin, Nup96. J. Cell Biol. **144:** 1097–1112.

Fornara, F., Panigrahi, K.C., Gissot, L., Sauerbrunn, N., Rühl, M., Jarillo, J.A., and Coupland, G. (2009). Arabidopsis DOF transcription factors act redundantly to reduce CONSTANS expression and are essential for a photoperiodic flowering response. Dev. Cell **17:** 75–86.

Gong, Z., Dong, C.H., Lee, H., Zhu, J., Xiong, L., Gong, D., Stevenson, B., and Zhu, J.K. (2005). A DEAD box RNA helicase is essential for mRNA export and important for development and stress responses in Arabidopsis. Plant Cell **17:** 256–267.

González-Aguilera, C., and Askjaer, P. (2012). Dissecting the NUP107 complex: Multiple components and even more functions. Nucleus **3:** 340–348.

Hayama, R., Sarid-Krebs, L., Richter, R., Fernández, V., Jang, S., and Coupland, G. (2017). PSEUDO RESPONSE REGULATORs stabilize CONSTANS protein to promote flowering in response to day length. EMBO J. **36:** 904–918.

Imaizumi, T., Schultz, T.F., Harmon, F.G., Ho, L.A., and Kay, S.A. (2005). FKF1 F-box protein mediates cyclic degradation of a repressor of CONSTANS in Arabidopsis. Science **309:** 293–297.

Ishitani, M., Xiong, L., Lee, H., Stevenson, B., and Zhu, J.K. (1998). HOS1, a genetic locus involved in cold-responsive gene expression in Arabidopsis. Plant Cell **10:** 1151–1161.

Ito, S., Song, Y.H., Josephson-Day, A.R., Miller, R.J., Breton, G., Olmstead, R.G., and Imaizumi, T. (2012). FLOWERING BHLH transcriptional activators control expression of the photoperiodic flowering regulator CONSTANS in Arabidopsis. Proc. Natl. Acad. Sci. USA **109:** 3582–3587.

Iwamoto, M., Asakawa, H., Hiraoka, Y., and Haraguchi, T. (2010). Nucleoporin Nup98: A gatekeeper in the eukaryotic kingdoms. Genes Cells **15:** 661–669.

Jacob, Y., Mongkolsiriwatana, C., Veley, K.M., Kim, S.Y., and Michaels, S.D. (2007). The nuclear pore protein AtTPR is required for RNA homeostasis, flowering time, and auxin signaling. Plant Physiol. **144:** 1383–1390.

Jang, S., Marchal, V., Panigrahi, K.C., Wenkel, S., Soppe, W., Deng, X.W., Valverde, F., and Coupland, G. (2008). Arabidopsis COP1 shapes the temporal pattern of CO accumulation conferring a photoperiodic flowering response. EMBO J. **27:** 1277–1288.

Jarillo, J.A., and Piñeiro, M. (2011). Timing is everything in plant development: The central role of floral repressors. Plant Sci. **181:** 364–378.

Jung, J.H., Park, J.H., Lee, S., To, T.K., Kim, J.M., Seki, M., and Park, C.M. (2013). The cold signaling attenuator HIGH EXPRESSION OF OSMOTICALLY RESPONSIVE GENE1 activates FLOWERING LOCUS C transcription via chromatin remodeling under short-term cold stress in Arabidopsis. Plant Cell **25:** 4378–4390.

Jung, J.H., Seo, P.J., and Park, C.M. (2012). The E3 ubiquitin ligase HOS1 regulates Arabidopsis flowering by mediating CONSTANS degradation under cold stress. J. Biol. Chem. **287:** 43277–43287.

Kim, W.Y., Fujiwara, S., Suh, S.S., Kim, J., Kim, Y., Han, L., David, K., Putterill, J., Nam, H.G., and Somers, D.E. (2007). ZEITLUPE is a circadian photoreceptor stabilized by GIGANTEA in blue light. Nature **449:** 356–360.

Koornneef, M., Alonso-Blanco, C., Blankestijn-de Vries, H., Hanhart, C.J., and Peeters, A.J. (1998). Genetic interactions among late-flowering mutants of Arabidopsis. Genetics **148:** 885–892.

Kubota, A., et al. (2017). TCP4-dependent induction of CONSTANS transcription requires GIGANTEA in photoperiodic flowering in Arabidopsis. PLoS Genet. **13:** e1006856.

Laubinger, S., Marchal, V., Le Gourrierec, J., Wenkel, S., Adrian, J., Jang, S., Kulajta, C., Braun, H., Coupland, G., and Hoecker, U. (2006). Arabidopsis SPA proteins regulate photoperiodic flowering and interact with the floral inducer CONSTANS to regulate its stability. Development **133:** 3213–3222.

Lazaro, A., Mouriz, A., Piñeiro, M., and Jarillo, J.A. (2015). Red light-mediated degradation of CONSTANS by the E3 ubiquitin ligase HOS1 regulates photoperiodic flowering in Arabidopsis. Plant Cell **27:** 2437–2454.

Lazaro, A., Valverde, F., Piñeiro, M., and Jarillo, J.A. (2012). The Arabidopsis E3 ubiquitin ligase HOS1 negatively regulates CONSTANS abundance in the photoperiodic control of flowering. Plant Cell **24:** 982–999.

Lee, H., Suh, S.S., Park, E., Cho, E., Ahn, J.H., Kim, S.G., Lee, J.S., Kwon, Y.M., and Lee, I. (2000). The AGAMOUS-LIKE 20 MADS domain protein integrates floral inductive pathways in Arabidopsis. Genes Dev. **14:** 2366–2376.

Lee, J.H., Kim, J.J., Kim, S.H., Cho, H.J., Kim, J., and Ahn, J.H. (2012). The E3 ubiquitin ligase HOS1 regulates low ambient temperature-responsive flowering in *Arabidopsis thaliana*. Plant Cell Physiol. **53:** 1802–1814.

Lee, K., and Seo, P.J. (2015). The E3 ubiquitin ligase HOS1 is involved in ethylene regulation of leaf expansion in Arabidopsis. Plant Signal. Behav. **10:** e1003755.

Liu, L.J., Zhang, Y.C., Li, Q.H., Sang, Y., Mao, J., Lian, H.L., Wang, L., and Yang, H.Q. (2008). COP1-mediated ubiquitination of CONSTANS is implicated in cryptochrome regulation of flowering in Arabidopsis. Plant Cell **20:** 292–306.

MacGregor, D.R., et al. (2013). HIGH EXPRESSION OF OSMOTICALLY RESPONSIVE GENES1 is required for circadian periodicity through the promotion of nucleo-cytoplasmic mRNA export in Arabidopsis. Plant Cell **25:** 4391–4404.

MacGregor, D.R., and Penfield, S. (2015). Exploring the pleiotropy of hos1. J. Exp. Bot. **66:** 1661–1671.

Marshall, C.M., Tartaglio, V., Duarte, M., and Harmon, F.G. (2016). The Arabidopsis *sickle* mutant exhibits altered circadian clock responses to cool temperatures and temperature-dependent alternative splicing. Plant Cell **28:** 2560–2575.

Meier, I., and Brkljacic, J. (2009). Adding pieces to the puzzling plant nuclear envelope. Curr. Opin. Plant Biol. **12:** 752–759.

Michaels, S.D. (2009). Flowering time regulation produces much fruit. Curr. Opin. Plant Biol. **12:** 75–80.

Murtas, G., Reeves, P.H., Fu, Y.F., Bancroft, I., Dean, C., and Coupland, G. (2003). A nuclear protease required for flowering-time regulation in Arabidopsis reduces the abundance of SMALL UBIQUITIN-RELATED MODIFIER conjugates. Plant Cell **15:** 2308–2319.

Parry, G. (2014). Components of the Arabidopsis nuclear pore complex play multiple diverse roles in control of plant growth. J. Exp. Bot. **65:** 6057–6067.

Parry, G., Ward, S., Cernac, A., Dharmasiri, S., and Estelle, M. (2006). The Arabidopsis SUPPRESSOR OF AUXIN RESISTANCE proteins are nucleoporins with an important role in hormone signaling and development. Plant Cell **18:** 1590–1603.

Rédei, G.P. (1962). Supervital mutants of Arabidopsis. Genetics **47:** 443–460.

Rothbauer, U., Zolghadr, K., Muyldermans, S., Schepers, A., Cardoso, M.C., and Leonhardt, H. (2008). A versatile nanotrap for biochemical and functional studies with fluorescent fusion proteins. Mol. Cell. Proteomics **7:** 282–289.

Ruan, W., Guo, M., Wang, X., Guo, Z., Xu, Z., Xu, L., Zhao, H., Sun, H., Yan, C., and Yi, K. (2019). Two RING-finger ubiquitin E3 ligases regulate the degradation of SPX4, an internal phosphate sensor, for phosphate homeostasis and signaling in rice. Mol. Plant **12:** 1060–1074.

Samach, A., Onouchi, H., Gold, S.E., Ditta, G.S., Schwarz-Sommer, Z., Yanofsky, M.F., and Coupland, G. (2000). Distinct roles of CONSTANS target genes in reproductive development of Arabidopsis. Science **288:** 1613–1616.

Sarid-Krebs, L., Panigrahi, K.C., Fornara, F., Takahashi, Y., Hayama, R., Jang, S., Tilmes, V., Valverde, F., and Coupland, G. (2015). Phosphorylation of CONSTANS and its COP1-dependent degradation during photoperiodic flowering of Arabidopsis. Plant J. **84:** 451–463.

Shen, L., Kang, Y.G., Liu, L., and Yu, H. (2011). The J-domain protein J3 mediates the integration of flowering signals in Arabidopsis. Plant Cell **23:** 499–514.

Shim, J.S., Kubota, A., and Imaizumi, T. (2017). Circadian clock and photoperiodic flowering in Arabidopsis: CONSTANS is a hub for signal integration. Plant Physiol. **173:** 5–15.

Song, Y.H., Estrada, D.A., Johnson, R.S., Kim, S.K., Lee, S.Y., MacCoss, M.J., and Imaizumi, T. (2014). Distinct roles of FKF1, Gigantea, and Zeitlupe proteins in the regulation of Constans stability in Arabidopsis photoperiodic flowering. Proc. Natl. Acad. Sci. USA **111:** 17672–17677.

Song, Y.H., Smith, R.W., To, B.J., Millar, A.J., and Imaizumi, T. (2012). FKF1 conveys timing information for CONSTANS stabilization in photoperiodic flowering. Science **336:** 1045–1049.

Strambio-De-Castillia, C., Niepel, M., and Rout, M.P. (2010). The nuclear pore complex: Bridging nuclear transport and gene regulation. Nat. Rev. Mol. Cell Biol. **11:** 490–501.

Suárez-López, P., Wheatley, K., Robson, F., Onouchi, H., Valverde, F., and Coupland, G. (2001). CONSTANS mediates between the circadian clock and the control of flowering in Arabidopsis. Nature **410:** 1116–1120.

Tamura, K., Fukao, Y., Iwamoto, M., Haraguchi, T., and Hara-Nishimura, I. (2010). Identification and characterization of nuclear pore complex components in *Arabidopsis thaliana*. Plant Cell **22:** 4084–4097.

Tanaka, Y., Kimura, T., Hikino, K., Goto, S., Nishimura, M., Mano, S., and Nakagawa, T. (2012). Gateway vectors for plant genetic engineering: Overview of plant vectors, application for bimolecular fluorescence complementation (BiFC) and multigene construction. In Genetic Engineering: Basics, New Applications and Responsibilities, H. Barrera-Saldaña, ed (London: IntechOpen), pp. 35–58.

Tran, E.J., and Wente, S.R. (2006). Dynamic nuclear pore complexes: Life on the edge. Cell **125:** 1041–1053.

Valverde, F., Mouradov, A., Soppe, W., Ravenscroft, D., Samach, A., and Coupland, G. (2004). Photoreceptor regulation of CONSTANS protein in photoperiodic flowering. Science **303:** 1003–1006.

Wälde, S., and Kehlenbach, R.H. (2010). The part and the whole: Functions of nucleoporins in nucleocytoplasmic transport. Trends Cell Biol. **20:** 461–469.

Wang, Q., Barshop, W.D., Bian, M., Vashisht, A.A., He, R., Yu, X., Liu, B., Nguyen, P., Liu, X., Zhao, X., Wohlschlegel, J.A., and Lin, C. (2015). The blue light-dependent phosphorylation of the CCE domain determines the photosensitivity of Arabidopsis CRY2. Mol. Plant **8:** 631–643.

Wang, X., Fan, C., Zhang, X., Zhu, J., and Fu, Y.F. (2013). BioVector, a flexible system for gene specific-expression in plants. BMC Plant Biol. **13:** 198.

Weigel, D., Alvarez, J., Smyth, D.R., Yanofsky, M.F., and Meyerowitz, E.M. (1992). LEAFY controls floral meristem identity in Arabidopsis. Cell **69:** 843–859.

Wigge, P.A., Kim, M.C., Jaeger, K.E., Busch, W., Schmid, M., Lohmann, J.U., and Weigel, D. (2005). Integration of spatial and temporal information during floral induction in Arabidopsis. Science **309:** 1056–1059.

Xu, X.M., Rose, A., Muthuswamy, S., Jeong, S.Y., Venkatakrishnan, S., Zhao, Q., and Meier, I. (2007). NUCLEAR PORE ANCHOR, the Arabidopsis homolog of Tpr/Mlp1/Mlp2/megator, is involved in mRNA export and SUMO homeostasis and affects diverse aspects of plant development. Plant Cell **19:** 1537–1548.

Yoo, S.K., Chung, K.S., Kim, J., Lee, J.H., Hong, S.M., Yoo, S.J., Yoo, S.Y., Lee, J.S., and Ahn, J.H. (2005). CONSTANS activates SUPPRESSOR OF OVEREXPRESSION OF CONSTANS 1 through FLOWERING LOCUS T to promote flowering in Arabidopsis. Plant Physiol. **139:** 770–778.

Zhang, Y., and Li, X. (2005). A putative nucleoporin 96 is required for both basal defense and constitutive resistance responses mediated by suppressor of *npr1-1,constitutive 1*. Plant Cell **17:** 1306–1316.

Zhao, Q., and Meier, I. (2011). Identification and characterization of the Arabidopsis FG-repeat nucleoporin Nup62. Plant Signal. Behav. **6:** 330–334.